156

McDonald, Jeffrey

om: McDonald, Jeffrey
nt: Wednesday, February 12, 2014 1:41 PM
o: 'Gilmore, Tyler J'
Cc: Bayer, MaryRose; Greenhagen, Andrew; Akhavan, Maryam; Krueger, Thomas; McAuliffe, Mary
Subject: draft AOR plan
Attachments: AOR plan-Review-01152014.docx

Tyler,
There are so many pieces in motion, it is hard to give each the time they deserve. We thought that giving you this draft now with some of our comments and observations (below) would help move things along faster.
Jeff

Regarding the AOR plan:

- Pg. 3; figure needs to reflect revised injection zone (including the lower Lombard) or the graphic could be eliminated.
- Confirmed injection interval depth with FGA. This is identified in graphics on pages 4, 7, 11, 13 (table 3.8), 15, and 16. The text on page 5 (1.2) needs to be changed to show the revised injection zone.
- Pg. 19; Gupta and Blair (1997) at the beginning of the last paragraph. Or is it Gupta and Bair?
- Pg. 20; Is the lack of regional groundwater flow map something that has to be addressed now or is it of limited value?
- Pg. 27; AOR delineation method needs to be inserted here, however, we are still evaluating it.
- Pg. 29; Although I agree that a quantitative threshold makes sense, I thought that we had struggled concept. What is an appropriate threshold? I'll look at the guidance in case I'm forgetting something from that.
- Pg. 29; As far as a schedule to reevaluate, can the FGA propose something?
- Pg. 29; I agree with the seismic event or other emergency, but I think we would have to be explicit about what magnitude or type of emergency.

Jeffrey R. McDonald, Geologist
Underground Injection Control Branch
U.S. EPA - Region 5
(312) 353-6288 [office]
(312) 408-2240 [direct fax]
mcdonald.jeffrey@epa.gov

Area of Review and Corrective Action Plan

Facility Information

Facility name: Alliance, the FutureGen 2.0

Facility contacts (names, titles, phone numbers, email addresses):
FutureGen Industrial Alliance, Inc.
73 Central Park Plaza East
Jacksonville, IL 62650
Telephone: 217/243-8215
Email: info@FutureGenAlliance.org
Homepage: www.FutureGenAlliance.org

Location (town/county/etc.): Morgan County, Illinois

Computational Modeling

Model Name: STOMP-CO2 simulator
Model Authors/Institution: White et al. 2012; White and Oostrom 2006; White and McGrail 2005 / Pacific Northwest National Laboratory (PNNL)
Description of model:
The simulations conducted for this investigation were executed using the STOMP-CO2 simulator (White et al. 2012; White and Oostrom 2006; White and Oostrom 2000). STOMP-CO2 was verified against other codes used for simulation of geologic disposal of CO_2 as part of the GeoSeq code intercomparison study (Pruess et al. 2002).

Partial differential conservation equations for fluid mass, energy, and salt mass compose the fundamental equations for STOMP-CO2. Coefficients within the fundamental equations are related to the primary variables through a set of constitutive relationships. The salt transport equations are solved simultaneously with the component mass and energy conservation equations. The solute and reactive species transport equations are solved sequentially after the coupled flow and transport equations. The fundamental coupled flow equations are solved using an integral volume finite-difference approach with the nonlinearities in the discretized equations resolved through Newton-Raphson iteration. The dominant nonlinear functions within the STOMP-CO2 simulator are the relative permeability-saturation-capillary pressure (k-s-p) relationships.
The STOMP-CO2 simulator allows the user to specify these relationships through a large variety of popular and classic functions. Two-phase (gas-aqueous) k-s-p relationships can be specified with hysteretic or nonhysteretic functions or nonhysteretic tabular data. Entrapment of CO_2 with imbibing water conditions can be modeled with the hysteretic two-phase k-s-p functions. Two-phase k-s-p relationships span both saturated and unsaturated conditions. The aqueous phase is assumed to never completely disappear through extensions to the s-p function below the residual saturation and a vaporpressure lowering scheme. Supercritical CO_2 has the function of a gas I these two-phase k-s-p relationships.

For the range of temperature and pressure conditions present in deep saline reservoirs, four phases are possible: 1) water-rich liquid (aqueous), 2) CO_2-rich vapor (gas), 3) CO_2-rich liquid (liquid-CO_2), and 4) crystalline salt (precipitated salt). The equations of state express 1) the existence of phases given the temperature, pressure, and water, CO_2, and salt concentration; 2) the partitioning of components among existing phases; and 3) the density of the existing phases.

Thermodynamic properties for CO_2 are computed via interpolation from a property data table stored in an external file. The property table was developed from the equation of state for CO_2 published by Span and Wagner (1996). Phase equilibria calculations in STOMP-CO2 use the formulations of Spycher et al. (2003) for temperatures below 100°C and Spycher and Pruess (2010) for temperatures above 100°C, with corrections for dissolved salt provided in Spycher and Pruess (2010). The Spycher formulations are based on the Redlich-Kwong equation of state with parameters fitted from published experimental data for CO_2-H_2O systems. Additional details regarding the equations of state used in STOMP-CO2 can be found in the guide by White et al. (2012)

A well model is defined as a type of source term that extends over multiple grid cells, where the well diameter is smaller than the grid cell. A fully coupled well model in STOMP-CO2 was used to simulate the injection of $scCO_2$ under a specified mass injection rate, subject to a pressure limit. When the mass injection rate can be met without exceeding the specified pressure limit, the well is considered to be flow controlled. Conversely, when the mass injection rate cannot be met without exceeding the specified pressure limit, the well is considered to be pressure controlled and the mass injection rate is determined based on the injection pressure. The well model assumes a constant pressure gradient within the well and calculates the injection pressure at each cell in the well. The CO_2 injection rate is proportional to the pressure gradient between the well and surrounding formation in each grid cell. By fully integrating the well equations into the reservoir field equations, the numerical convergence of the nonlinear conservation and constitutive equations is greatly enhanced.

Model Inputs and Assumptions:

1. Model Domain

1.1 Site Geology

The regional geology of Illinois is well known from wells and borings drilled in conjunction with hydrocarbon exploration, aquifer development and use, and coal and commercial mineral exploration. Related data are largely publicly available through the Illinois State Geological Survey (ISGS)[1] and the U.S. Geological Survey (USGS)[2]. In addition, the DOE has sponsored a number of studies by the Midwest Geologic Sequestration Consortium[3] to evaluate subsurface strata in Illinois and adjacent states as possible targets for the containment of anthropogenic CO_2 (Figure 1- (Figure 2.1)).

To support the evaluation of the Morgan County site as a potential carbon storage site a deep stratigraphic well was drilled and extensively characterized. The stratigraphic well, located at longitude 90.0528W, latitude 39.8067N, is approximately 1 mi (1.6 km) east of the planned storage site. The stratigraphic well reached a total depth of 4,826 ft (1,471 m) bgs within the Precambrian basement. The well penetrated 479 ft (146 m) of the Eau Claire Formation and 512 ft (156 m) of the Mount Simon Sandstone. The stratigraphic well was extensively characterized, sampled, and geophysically logged during drilling. A total of 177 ft of whole core were collected from the lower Eau Claire-upper Mount Simon Sandstone and 34 ft were collected from lower Mount Simon Sandstone-Precambrian basement interval. In addition to whole drill core, a total of 130 side-wall core plugs were obtained from the combined interval of the Eau Claire Formation, Mount Simon Sandstone, and the Precambrian basement. In Figure 2 (Figure 2.11), cored

[1] http://www.isgs.uiuc.edu/
[2] http://www.usgs.gov/
[3] http://sequestration.org/

intervals are indicated with red bars; rotary side-wall core and core-plug locations are indicated to the left of the lithology panel. Standard gamma ray and resistivity curves are shown in the second panel. The proposed injection interval (location of the horizontal wells' injection laterals) is highlighted on the geophysical log panels in Figure 2.

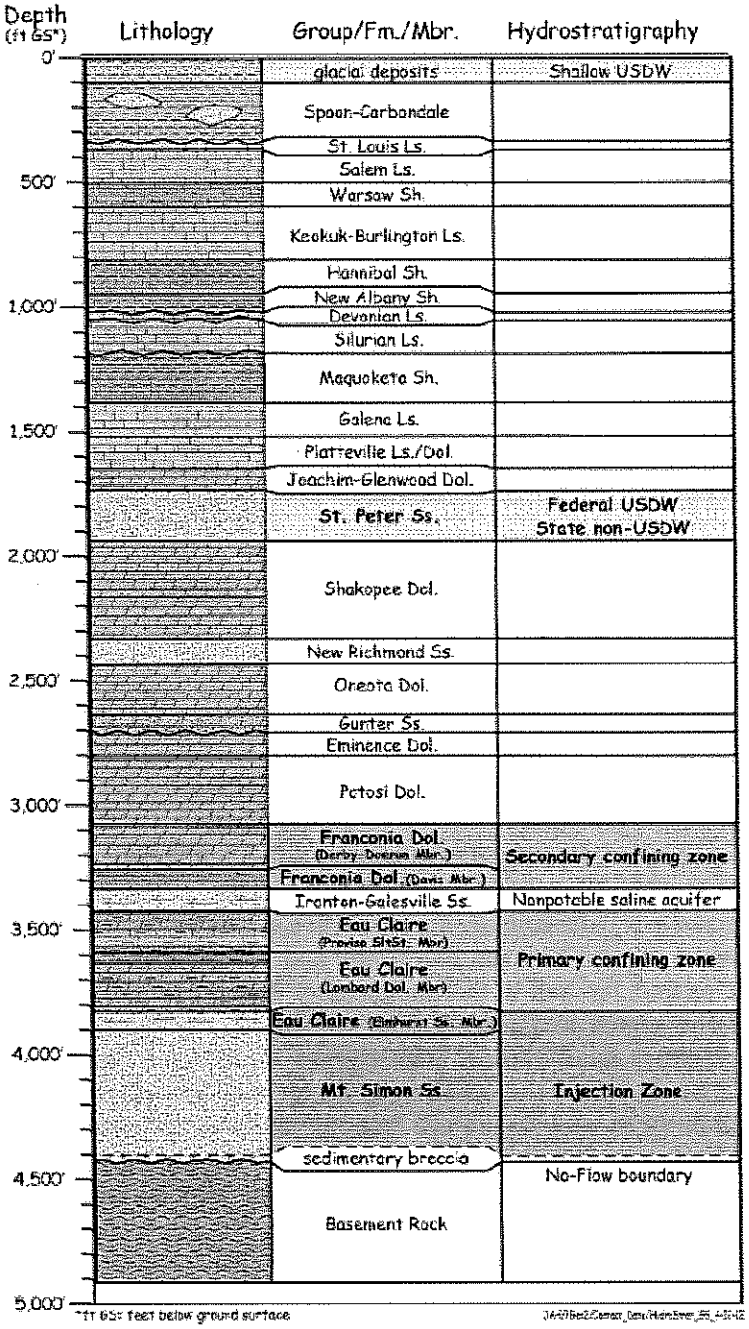

Stratigraphy and Proposed Injection and Confining Zones at the Morgan County CO_2 Storage Site

Figure 1

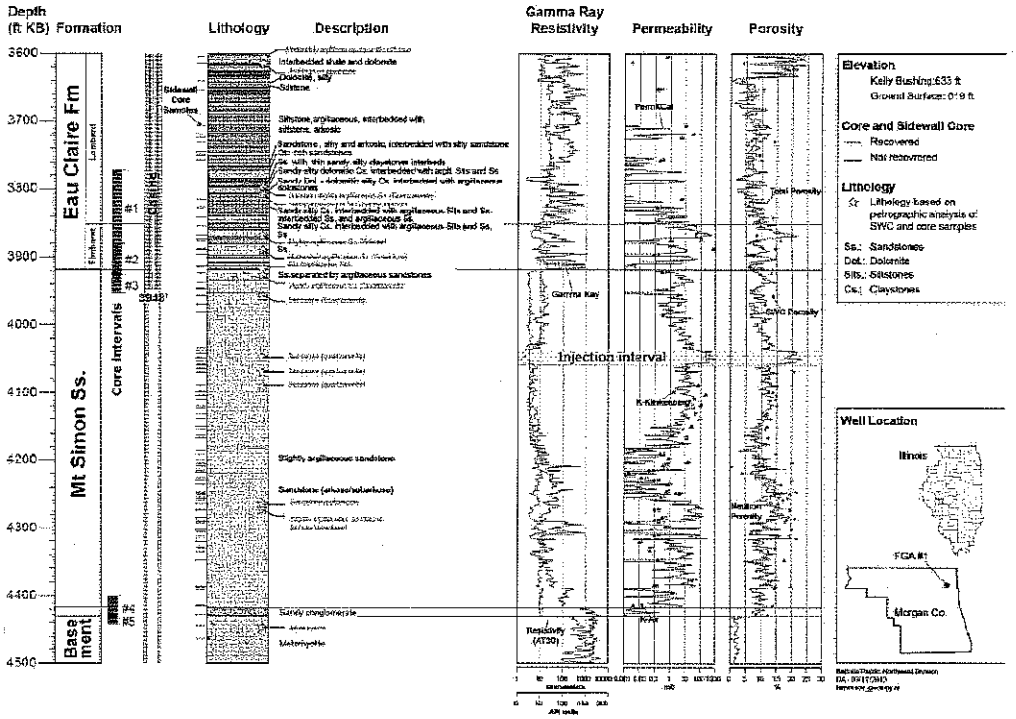

Figure 2.11. Lithology, Mineralogy, and Hydrologic Units of the Proposed Injection Zone (Mt Simon and Elmhurst) and Lower Primary Confining Zone (Lombard), as Encountered Within the Stratigraphic Well. Data are explained in the text.

Figure 2

1.1.1 Seismic profile

Two two-dimensional (2D) surface seismic lines, shown in Figure 3 (Figure 2.14), were acquired in January 2011 along public roads near the proposed Morgan County CO_2 storage site. The seismic lines are not of optimal quality due to seismic noise, but they do not indicate the presence of obvious faults or large changes in thickness of the injection or confining zones. Both profiles indicate a thick sequence of Paleozoic-aged rocks with a contact between Precambrian and Mount Simon at 640 ms and a contact between Eau Claire and Mount Simon at 580 ms. Some vertical disruptions, which extend far below the sedimentary basin, remain and their regular spatial periodicity is unlikely related to faults. A fault can usually be recognized and interpreted in seismic data if it creates a quasi-vertical displacement of 20 ms or more in several successive reflection events. The amount of vertical fault throw that would produce a 20-ms vertical displacement would be (0.01 sec) X (P-wave interval velocity), for whatever interval velocity is appropriate local to a suspected fault. For the interval from the surface down to the Eau Claire at the FutureGen site in Morgan County, the P-wave interval velocity local to seismic lines L101 and L201 ranges from approximately 7,000 ft/s (shallow) to approximately 12,000 ft/s (deep). Thus, faults having vertical throws of 120 ft at the Eau Claire, and perhaps as little as 70 ft at shallow depths, should be detected if they traverse either profile. No faults with a clear vertical displacement have been identified; the only clear observation that can be made is the existence of a growth fault that affects Mount Simon and Eau Claire formations in the eastern part of the L201 profile at offset 28,000 ft. This growth fault is more than 1.5 miles away from the outermost edge of the CO_2 plume and does not extend far upward in the overburden. For these reasons, it is highly unlikely that it could affect the integrity of the reservoir. The closest known earthquake to the FutureGen 2.0 Project site (Intensity VII, magnitude 4.8 – non-instrumented record) occurred on July 19, 1909, approximately 28 mi (45 km) north of the site; it caused slight damage. Most of

the events in Illinois occurred at depths greater than 3 km (1.9 mi). ISGS recently acquired a new 120-mi long seismic reflection survey across central Illinois as part of a DOE-sponsored research project to characterize reservoir rocks for geologic storage of carbon dioxide. The continuous east-west line extends from Meredosia to southwestern Champaign County (Figure 3). This line, which is currently under re-processing, will supply additional information about the structure of the sedimentary layers which will be correlated to the observations made on both profiles L101 and L201.

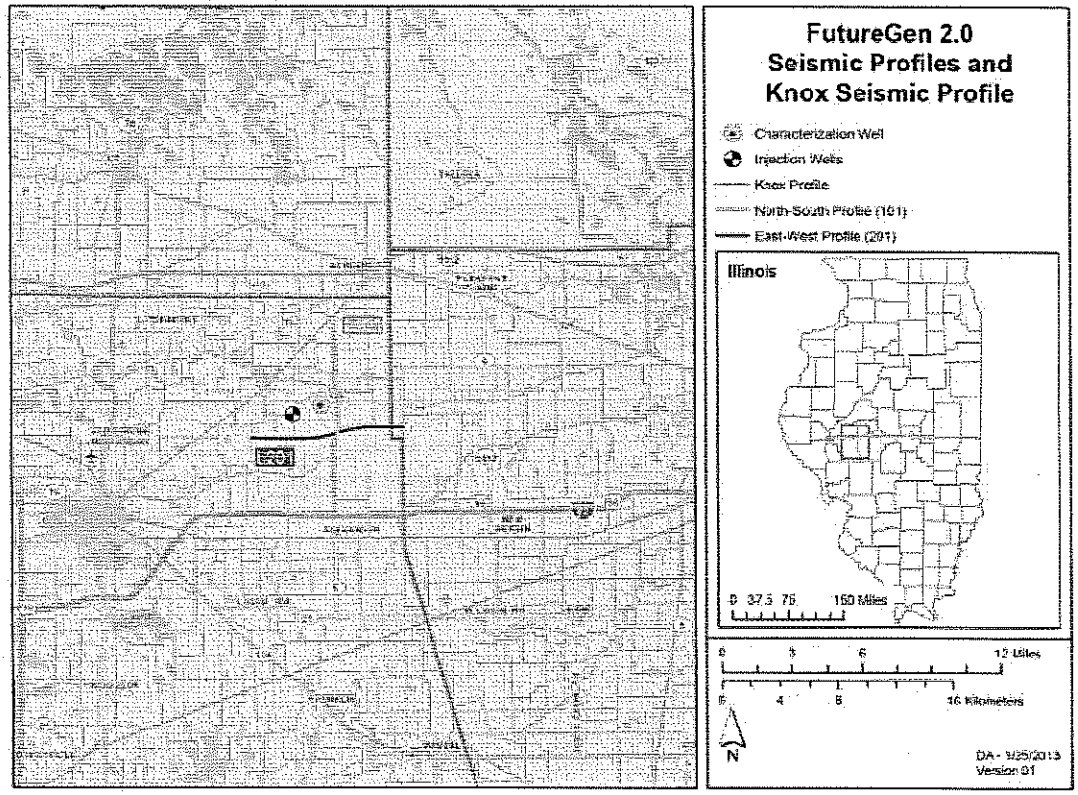

Figure 2.14. Location of the two 2D seismic survey lines, L101 and L201, at the proposed Morgan County CO_2 storage site. The north-south line is along Illinois State Highway 123. The Knox seismic profile completed in 2012 by the ISGS and that passes within 10 miles of the site is also drawn in orange.

Figure 3

1.2 Conceptual model

A stratigraphic conceptual model of the geologic layers from the Precambrian basement to ground surface was constructed using the EarthVision® software package. The model domain for the Morgan County CO_2 storage site consists of the injection zone (Mount Simon and Elmhurst), the primary confining zone (Lombard and Proviso), the Ironton-Galesville, and the secondary confining zone (Davis-Ironton and the Franconia). Borehole data from the FutureGen 2.0 stratigraphic well and data from regional boreholes and published regional contour maps were used as input data. However, units below the Shakopee Dolomite and above the Eau Claire Formation were assumed to have a constant thickness based on the stratigraphy observed at the stratigraphic well. There is a regional dip of approximately 0.25 degrees in the east-southeast direction. Preliminary simulations were conducted to determine the extent of the model domain so that lateral boundaries were distant enough from the injection location so as not to influence the model results and an expanded 100- x 100-mi conceptual model was constructed. These

surfaces were gridded in EarthVision® based on borehole data and regional contour maps and make up the stratigraphic layers of the computational model. The three dimensional, boundary-fitted numerical model grid was designed to have constant grid spacing with higher resolution in the area influenced by the CO_2 injection (3- by 3-mi area), with increasingly larger grid spacing moving out in all lateral directions toward the domain boundary.

The conceptual model hydrogeologic layers were defined for each stratigraphic layer based on zones of similar hydrologic properties. The hydrologic properties (permeability, porosity) were deduced from geophysical well logs and side-wall cores. The lithology, deduced from wireline logs and core data, was also used to subdivide each stratigraphic layer of the model. Based on these data, the Mount Simon Sandstone was subdivided into 17 layers, and the Elmhurst Sandstone (member of the Eau Claire Formation) was subdivided into 7 layers (Figure 4- (Figure 3.2)). These units form the injection zone. The Lombard and Proviso members of the Eau Claire Formation were subdivided respectively into 14 and 5 layers. The Ironton Sandstone was divided into four layers, the Davis Dolomite into three layers, and the Franconia Formation into one layer. Some layers ("split" label in Figure 4) have similar properties but have been subdivided to maintain a reasonable thickness of layers within the injection zone as represented in the computational model. The thickness of the layers varies from 4 to 172 ft, with an average of 26 ft. Figure 5 (Figure 3.14) shows the numerical model grid for the entire 100- by 100-mi domain and also for the 3- by 3-mi area with higher grid resolution and uniform grid spacing of 200 ft by 200 ft. The model grid contains 125 nodes in the x-direction, 125 nodes in the y-direction, and 51 nodes in the z-direction for a total number of nodes equal to 796,875. The expanded geologic model was queried at the node locations of the numerical model to determine the elevation of each surface for the stratigraphic units at the numerical model grid cell centers (nodes) and cell edges. Then each of those layers was subdivided into the model layers by scaling the thickness to preserve the total thickness of each stratigraphic unit. Once the vertical layering was defined, material properties were mapped to each node in the model.

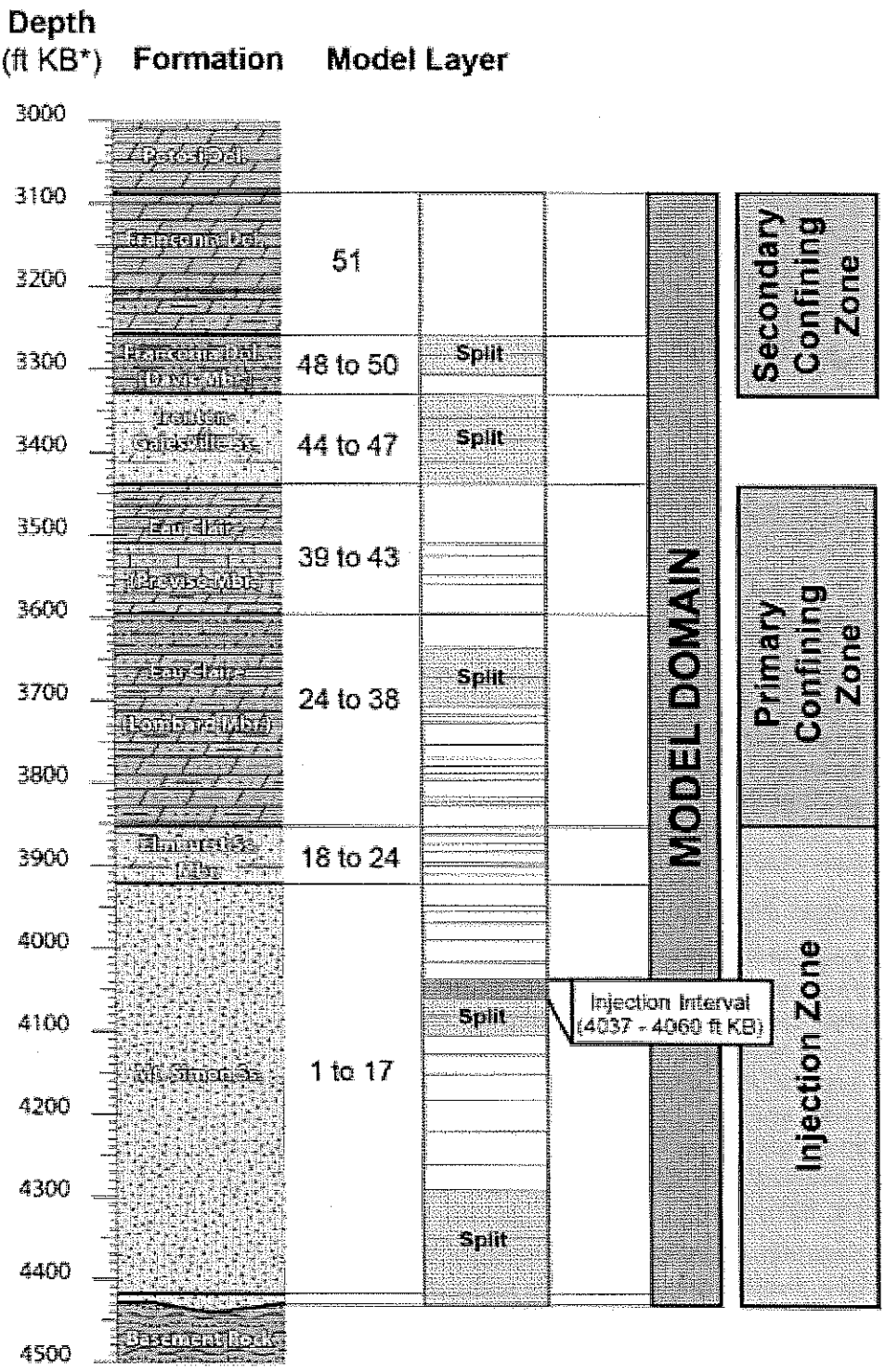

Division of Stratigraphic Layers to Create Computational Model Layers

Figure 4

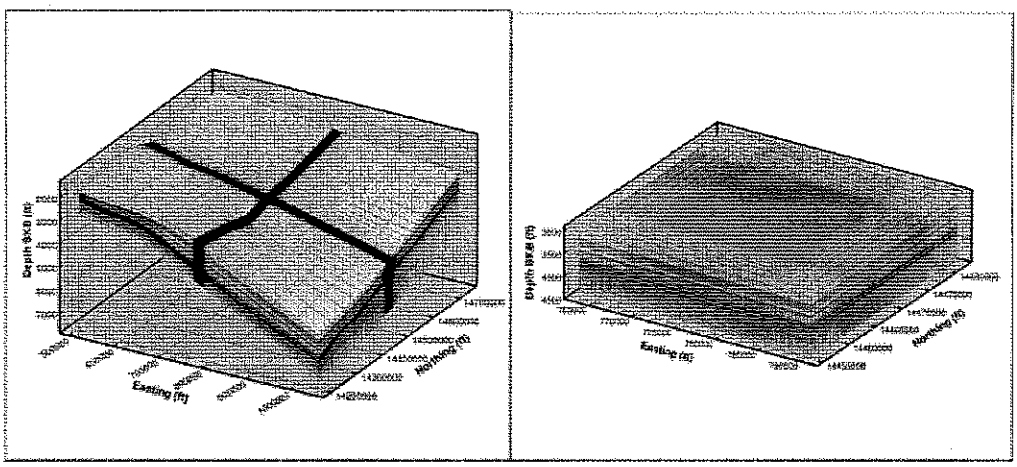

(a) (b)

Figure 3.14. Numerical Model Grid for a) Full Domain, and b) Finer Resolution Area Containing the Injection Wells

Figure 5

1.3 Simulation time period

Based on measured pressures in the alluvial aquifer system and the injection zone, it was determined that the pressure differential needed to force fluids from the injection zone into the surficial alluvial aquifer system through a hypothetical conduit was 31.45 psi. Therefore, once the pressure differential in the injection zone falls below this value, the simulation time period conditions are satisfied. The preliminary simulations show that by year 60 the pressure differential is below 30 psi at the location of the injection well. Hence, the final representative case simulations were executed for a period of 100 years.

2. Processes Modeled

Physical processes modeled in the reservoir simulations included isothermal multi-fluid flow and transport for a number of components (e.g., water, salt, and CO2) and phases (e.g., aqueous and gas). Isothermal conditions were modeled because it was assumed that the temperature of the injected CO2 will be similar to the formation temperature. Reservoir salinity is considered in the simulations because salt precipitation can occur near the injection well in higher permeability layers as the rock dries out during CO2 injection. This can completely plug pore throats, making the layer impermeable, thereby reducing reservoir injectivity and affecting the distribution of CO2 in the reservoir. No porosity and permeability reduction due to salt precipitation was modeled (Input Advisory).

Injected CO_2 partitions in the reservoir between the free (or mobile) gas, entrapped gas, and aqueous phases. Sequestering CO_2 in deep saline reservoirs occurs through four mechanisms: 1) structural trapping, 2) aqueous dissolution, 3) hydraulic trapping, and 4) mineralization. Structural trapping is the long-term retention of the buoyant gas phase in the pore space of the reservoir rock held beneath one or more impermeable caprocks. Aqueous dissolution occurs when CO2 dissolves in the brine resulting in an aqueous-phase density greater than the ambient conditions. Hydraulic trapping is the pinch-off trapping of the gas phase in pores as the brine re-enters pore spaces previously occupied by the gas phase. Generally, hydraulic trapping only occurs upon the cessation of CO2 injection. Mineralization is the chemical reaction that transforms formation minerals to carbonate minerals. In the Mount Simon Sandstone, the most likely precipitation reaction is the formation of iron carbonate precipitates. A likely reaction

between CO2 and shale is the dewatering of clays. Laboratory investigations are currently quantifying the importance of these reactions at the Morgan County CO2 storage site. Based on its experiments, the FutureGen Alliance (the Alliance) expects to see a small mass of precipitates (KCl, NaCl) forming near the injection well from the scCO2 displacement of water, and does not expect to see the formation of any significant carbonate precipitates in this year (or years) time scale. Iron does precipitate, but concentrations are too low (<0.6 mmol/L) relative to carbonate mass to be a precipitate issue. Simulations by others (White et al. 2005) of scCO2 injection in a similar sandstone (also containing iron oxides) shows that over significantly longer time scales (1000+ years), alumino silicate dissolution and alumino silicate precipitation incorporating significant carbonate (dawsonite) is predicted, as well as precipitation of some calcite. That predicted mineral trapping did permanently sequester 21% of the carbonate mass, thus decreasing scCO2 transport risk (More details are presented in the response to NOD-December 10, 2013, Appendix A). Therefore, the simulations described here did not include mineralization reactions. However, the STOMP-CO2 simulator does account for precipitation of salt during CO2 injection. The CO2 stream provided by the plant to the storage site is no less than 97 percent dry basis CO2. Because the amount of impurities is small, for the purposes of modeling the CO2 injection and redistribution for this project, it was assumed that the injectate was pure CO2.

3. *Rock Properties*

3.1 Intrinsic Permeability

3.1.1 Site characterization

Permeability in the sandstones, as measured in rotary side-wall cores and plugs from whole core, appears to be dominantly related to grain size and abundance of clay. In Figure 2, ELAN-calculated permeability (red curve) is in the third panel, along with two different lab measurements of permeability for each rotary side-wall core. Horizontal permeability (Kh) data in the stratigraphic well outnumber vertical permeability (Kv) data, because Kh could not be determined from rotary side-wall cores. However, Kv/Kh ratios were successfully determined for 20 vertical/horizontal siliciclastic core-plug pairs cut from intervals of whole core. Within the Mount Simon Sandstone, the horizontal permeabilities of the lower Mount Simon alluvial fan lithofacies range from 0.005 to 0.006 mD and average ratios of vertical to horizontal permeabilities range from 0.635 to 0.722 (at the 4,318–4,388 ft KB depth, Figure 2). Horizontal core-plug permeabilities range from 0.032 to 2.34 mD at the 3,852–3,918 ft KB depth; Kv/Kh ratios for these same samples range from 0.081 to 0.833. The computed lithology track for the primary confining zone indicates the upward decrease in quartz silt and increase in carbonate in the Proviso member, along with a decrease in permeability. The permeabilities of the rotary side-wall cores in the Proviso range from 0.000005 mD to 1 mD. Permeabilities in the Lombard member range from 0.001 mD to 28 mD, reflecting the greater abundance of siltstone in this interval, particularly in the lowermost part of the member. Whole core plugs and associated vertical permeabilities are available only from the lowermost part of the Lombard. Thin (few inches/centimeters), high-permeability sandstone streaks resemble the underlying Elmhurst; low-permeability siltstone and mudstone lithofacies have vertical permeabilities of 0.0004-0.465 mD, and Kv/Kh ratios of 0.000 to 0.17. The ELAN geophysical logs indicated permeabilities are generally less than the wireline tool limit of 0.01 mD throughout the secondary confining zone. Two rotary side-wall cores were taken from the Franconia, and three side-wall cores were cut in the Davis member. Laboratory-measured rotary sidewall core (horizontal) permeabilities are very low (0.001–0.000005 mD). The permeabilities of the two Franconia samples were measured with a special pulse decay permeameter; the sample from 3,140 ft bgs (957 m) has a permeability less than the lower instrument limit of 0.000005 mD. Vertical core plugs are required for directly determining vertical permeability and there are no data from the stratigraphic well for vertical permeability or for determining vertical permeability anisotropy in the secondary confining zone.

However, Kv/Kh ratios of 0.007 have been reported elsewhere for Paleozoic carbonate mudstones (Saller et al. 2004).

3.1.2 Model Parameters

Intrinsic permeability data sources for the FutureGen 2.0 stratigraphic well include computed geophysical wireline surveys (CMR and ELAN logs), and where available, laboratory measurements of rotary SWCs, core plugs from the whole core intervals, and hydrologic tests (including wireline [MDT]), and packer tests. For model layers within the injection reservoir section (i.e., Elmhurst Sandstone and Mount Simon Sandstone; 3,852 to 4,432 ft [1174 to 1350 m]) wireline ELAN permeability model permKCal produced by Schlumberger (red curve on Figure 2). This model, calibrated by rotary side-wall and core plug permeabilities, provides a continuous permeability estimate over the entire injection reservoir section. This calibrated permeability response was then slightly adjusted, or scaled, to match the composite results obtained from the hydrologic packer tests over uncased intervals. For injection reservoir model layers within the cased well portion of the model, no hydrologic test data are available, and core-calibrated ELAN log response was used directly in assigning average model layer permeabilities. The hydraulic packer tests were conducted in two zones of the Mount Simon portion of the reservoir. The Upper Zone (3,948 ft bkb to 4,194 ft bkb) equates to layers 6 through 17 of the model, while the Lower Zone (4,200 ft bkb to 4,512 ft bkb) equates to layers 1 through 5. The most recent ELAN-based permeability-thickness product values are 9,524 mD-ft for the 246-ft-thick section of the upper Mount Simon corresponding to the Upper Zone and 3,139 mD-ft for the 312-ft-thick section of the lower Mount Simon corresponding to the Lower Zone. The total permeability-thickness product for the open borehole Mount Simon is 12,663 mD-ft, based on the ELAN logs. Results of the field hydraulic tests suggest that the upper Mount Simon permeability-thickness product is 9,040 mD-ft and the lower Mount Simon interval permeability-thickness product is 775 mD-ft. By simple direct comparison, the packer test for the upper Mount Simon is nearly equivalent (~95 percent) to the ELAN-predicted value, while the lower Mount Simon represents only ~25 percent of the ELAN-predicted value. Because no hydrologic test has been conducted in the Elmhurst Sandstone reservoir interval, a conservative scaling factor of 1 has been assigned to this interval, based on ELAN PermKCal data (The permeabilities used for this formation were the ELAN PermKCal values without applying a scaling factor). The sources of data for confining zones (Franconia to Lombard Formations) are similar to those for the injection zone reservoir, with the exception that no hydrologic or MDT test data are available. ELAN log-derived permeabilities are unreliable below about 0.01 mD (personal communication from Bob Butsch, Schlumberger, 2012). Because the average log-derived permeabilities (permKCal wireline from ELAN log) for most of the caprock layers are at or below 0.01 mD, an alternate approach was applied. For each model layer the core data were reviewed, and a simple average of the available horizontal Klinkenburg permeabilities was then calculated for each layer. Core samples that were noted as having potential cracks and/or were very small were eliminated if the results appeared to be unreasonable based on the sampled lithology. If no core samples were available and the arithmetic mean of the PermKCal was below 0.01 mD, a default value of 0.01 mD was applied (Lombard9 is the only layer with a 0.01-mD default value). Because the sandstone intervals of the Ironton-Galesville Sandstone have higher permeabilities that are similar in magnitude to the modeled reservoir layers, the Ironton-Galesville Sandstone model layer permeabilities were derived from the arithmetic mean of the PermKCal permeability curve. Because no hydraulic test has been conducted in the primary confining zone, the scaling factor was assigned to be 100 percent in this interval and the overburden formations. Figure 6 (Figure 3.3) shows the depth profile of the horizontal permeability assigned to each layer of the model and actual values assigned are listed in Table 1 (Table 3.8). Figure 7 (Figure 3.15) shows the distribution of horizontal and vertical permeability as it was assigned to the numerical model grid.

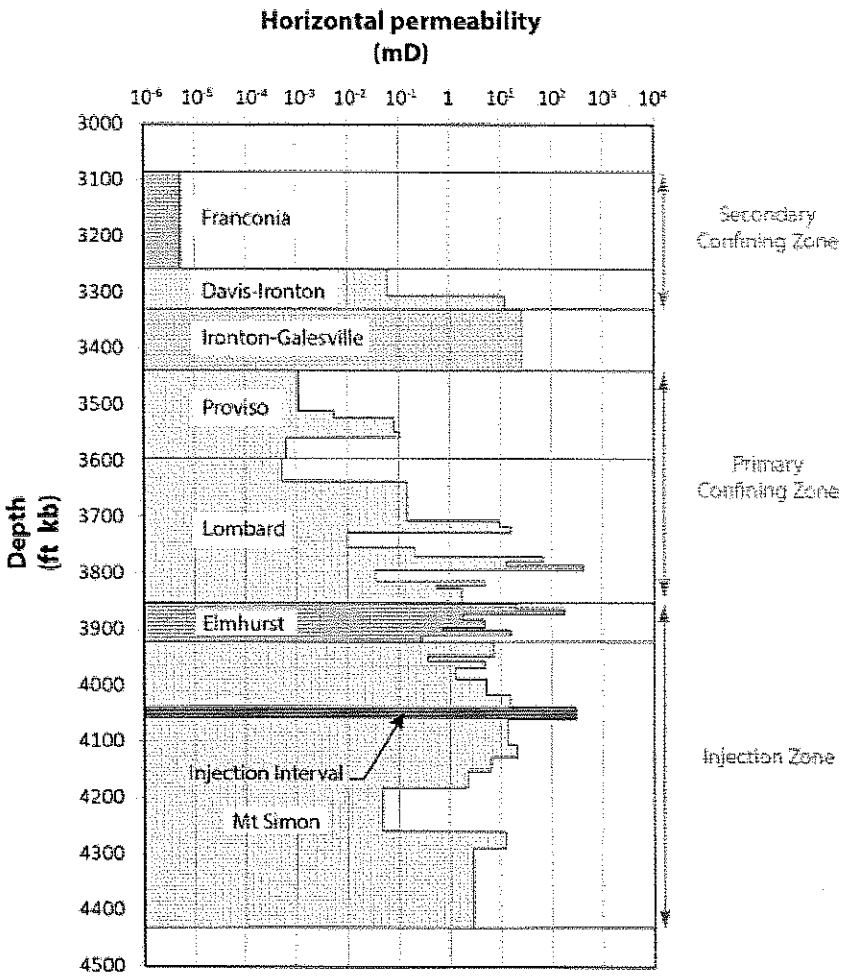

Figure 3.3. Horizontal Permeability Versus Depth in Each Model Layer
Figure 6

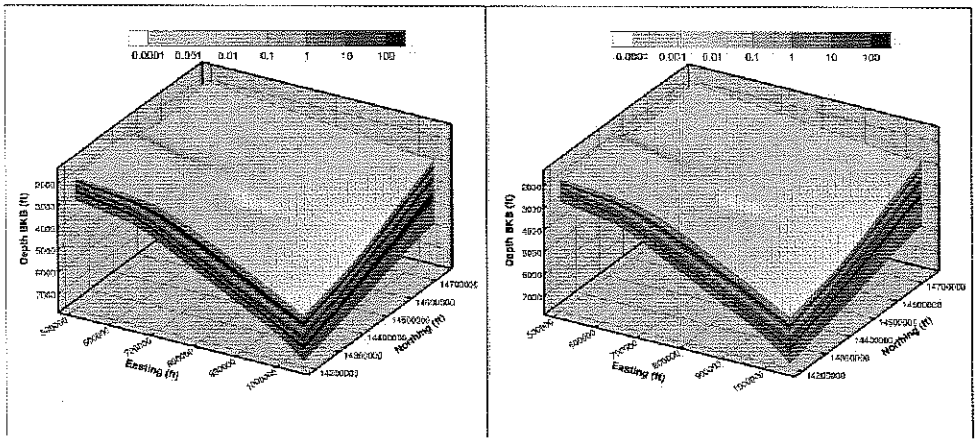

Figure 3.15. Permeability Assigned to Numerical Model a) Horizontal Permeability; b) Vertical Permeability

Figure 7

Table 1.

Table 3.8. Summary of the Hydrologic Properties Assigned to Each Model Layer

	Model Layer	Top Depth (ft bkb)	Top Elevation (ft)	Bottom Elevation (ft)	Thickness (ft)	Porosity	Horizontal Permeability (mD)	Vertical Permeability (mD)	Grain Density (g/cm3)	Compressibility (1/Pa)
Primary Conf. Zone	Franconia	3086.00	-2453	-2625	172	0.0358	5.50E-06	5.85E-08	2.82	7.42E-10
	Davis-Ironton3	3258.00	-2625	-2649	24	0.0367	6.26E-02	6.26E-03	2.73	3.71E-10
	Davis-Ironton2	3282.00	-2649	-2673	24	0.0367	6.26E-02	6.26E-03	2.73	3.71E-10
	Davis-Ironton1	3306.00	-2673	-2697	24	0.0218	1.25E+01	1.25E+00	2.73	3.71E-10
	Ironton-Galesville4	3330.00	-2697	-2725	28	0.0981	2.63E+01	1.05E+01	2.66	3.71E-10
	Ironton-Galesville3	3358.00	-2725	-2752	27	0.0981	2.63E+01	1.05E+01	2.66	3.71E-10
	Ironton-Galesville2	3385.00	-2752	-2779	27	0.0981	2.63E+01	1.05E+01	2.66	3.71E-10
	Ironton-Galesville1	3412.00	-2779	-2806	27	0.0981	2.63E+01	1.05E+01	2.66	3.71E-10
Primary Confining Zone	Proviso5	3439.00	-2806	-2877	71	0.0972	1.12E-03	1.12E-04	2.72	7.42E-10
	Proviso4	3510.00	-2877	-2891	14	0.0786	5.50E-03	5.50E-04	2.72	7.42E-10
	Proviso3	3524.00	-2891	-2916	25	0.0745	8.18E-02	5.73E-04	2.77	7.42E-10
	Proviso2	3548.50	-2916	-2926	10	0.0431	1.08E-01	7.56E-04	2.77	7.42E-10
	Proviso1	3558.50	-2926	-2963	38	0.0361	6.46E-04	4.52E-06	2.77	7.42E-10
	Lombard14	3596.00	-2963	-3003	40	0.1754	5.26E-04	5.26E-05	2.68	7.42E-10
	Lombard13	3636.00	-3003	-3038	35	0.0638	1.53E-01	1.53E-02	2.68	7.42E-10
	Lombard12	3671.00	-3038	-3073	35	0.0638	1.53E-01	1.53E-02	2.68	7.42E-10
	Lombard11	3706.00	-3073	-3084	11	0.0878	9.91E+00	9.91E-01	2.68	7.42E-10
	Lombard10	3717.00	-3084	-3094	10	0.0851	1.66E+01	1.66E+00	2.68	7.42E-10
	Lombard9	3727.00	-3094	-3121	27	0.0721	1.00E-02	1.00E-03	2.68	7.42E-10
	Lombard8	3753.50	-3121	-3138	17	0.0663	2.13E-01	2.13E-02	2.68	7.42E-10
	Lombard7	3770.50	-3138	-3145	8	0.0859	7.05E+01	7.05E+00	2.68	7.42E-10
	Lombard6	3778.00	-3145	-3153	8	0.0459	1.31E+01	1.31E+00	2.68	7.42E-10
	Lombard5	3785.50	-3153	-3161	9	0.0760	4.24E+02	4.24E+01	2.68	7.42E-10
	Lombard4	3794.00	-3161	-3181	20	0.0604	3.56E-02	3.56E-03	2.68	7.42E-10
	Lombard3	3814.00	-3181	-3189	8	0.0799	5.19E+00	5.19E-01	2.68	7.42E-10
	Lombard2	3821.50	-3189	-3194	5	0.0631	5.71E-01	5.71E-02	2.68	7.42E-10
	Lombard1	3826.50	-3194	-3219	26	0.0900	1.77E+00	1.77E-01	2.68	7.42E-10

Table 3.8. (contd)

Model Layer	Top Depth (ft bkb)	Top Elevation (ft)	Bottom Elevation (ft)	Thickness (ft)	Porosity	Horizontal Permeability (mD)	Vertical Permeability (mD)	Grain Density (g/cm3)	Compressibility (1/Pa)
Elmhurst7	3852.00	-3219	-3229	10	0.1595	2.04E+01	8.17E+00	2.64	3.71E-10
Elmhurst6	3862.00	-3229	-3239	10	0.1981	1.84E+02	7.38E+01	2.64	3.71E-10
Elmhurst5	3872.00	-3239	-3249	10	0.0822	1.87E+00	1.87E-01	2.64	3.71E-10
Elmhurst4	3882.00	-3249	-3263	14	0.1105	4.97E+00	1.99E+00	2.64	3.71E-10
Elmhurst3	3896.00	-3263	-3267	4	0.0768	7.52E-01	7.52E-02	2.64	3.71E-10
Elmhurst2	3900.00	-3267	-3277	10	0.1291	1.63E+01	6.53E+00	2.64	3.71E-10
Elmhurst1	3910.00	-3277	-3289	12	0.0830	2.90E-01	2.90E-02	2.64	3.71E-10
MtSimon17	3922.00	-3289	-3315	26	0.1297	7.26E+00	2.91E+00	2.65	3.71E-10
MtSimon16	3948.00	-3315	-3322	7	0.1084	3.78E-01	3.78E-02	2.65	3.71E-10
MtSimon15	3955.00	-3322	-3335	13	0.1276	5.08E+00	2.03E+00	2.65	3.71E-10
MtSimon14	3968.00	-3335	-3355	20	0.1082	1.33E+00	5.33E-01	2.65	3.71E-10
MtSimon13	3988.00	-3355	-3383	28	0.1278	5.33E+00	2.13E+00	2.65	3.71E-10
MtSimon12	4016.00	-3383	-3404	21	0.1473	1.59E+01	6.34E+00	2.65	3.71E-10
MtSimon11 (Injection Zone)	4037.00	-3404	-3427	23	0.2042	3.10E+02	1.55E+02	2.65	3.71E-10
MtSimon10	4060.00	-3427	-3449	22	0.1434	1.39E+01	4.18E+00	2.65	3.71E-10
MtSimon9	4082.00	-3449	-3471	22	0.1434	1.39E+01	4.18E+00	2.65	3.71E-10
MtSimon8	4104.00	-3471	-3495	24	0.1503	2.10E+01	6.29E+00	2.65	3.71E-10
MtSimon7	4128.00	-3495	-3518	23	0.1311	6.51E+00	1.95E+00	2.65	3.71E-10
MtSimon6	4151.00	-3518	-3549	31	0.1052	2.26E+00	6.78E-01	2.65	3.71E-10
MtSimon5	4182.00	-3549	-3588	39	0.1105	4.83E-02	4.83E-03	2.65	3.71E-10
MtSimon4	4221.00	-3588	-3627	39	0.1105	4.83E-02	4.83E-03	2.65	3.71E-10
MtSimon3	4260.00	-3627	-3657	30	0.1727	1.25E+01	1.25E+00	2.65	3.71E-10
MtSimon2	4290.00	-3657	-3717	60	0.1157	2.87E+00	2.87E-01	2.65	3.71E-10
MtSimon1	4350.00	-3717	-3799	82	0.1157	2.87E+00	2.87E-01	2.65	3.71E-10

3.2 Porosity

Total (or absolute) porosity is the ratio of void space to the volume of whole rock. Effective porosity is the ratio of interconnected void space to the volume of the whole rock. As a first step in assigning porosity values for the FutureGen 2.0 numerical model layers, Schlumberger ELAN porosity log results were compared with laboratory measurements of porosity as determined from SWC and core plugs for specific sampling depth within the Mount Simon. The Schlumberger ELAN porosity logs examined include PIGN (Gamma-Neutron Porosity), PHIT (Total Porosity), and PIGE (Effective Porosity). The PIGN and PIGE wireline log surveys use different algorithms to identify clay- or mineral-bound fluid/porosity in calculating an effective porosity value. SWC porosity measurements are listed as "total porosity," but their measurement can be considered to be determinations of "effective porosity," because the measurement technique (weight measurements of heated/oven-dried core samples) primarily measures the amount of "free" or connected pore liquid contained within the SWC sample as produced by the heating process. It should be noted that the SWC porosity measurements were determined under ambient pressure conditions. In Figure 2, neutron- and density-crossplot porosity is shown in the fourth panel, along with lab-measured porosity for core plugs and rotary side-wall cores. An available porosity measurement data set for a conventional Mount Simon core plug sample taken near the top of the formation (depth 3,926 ft) indicates only minor changes in porosity for measurements taken over a wide range in pressure (i.e., ambient to 1,730 psi). This suggests that ambient SWC porosity measurements of the Mount Simon may be representative of in situ formation pore pressure conditions. The ELAN porosity log results generally underestimate the SWC porosity measured values. As a result of the poor visual correlation of the PIGE survey results with SWC measurements, this ELAN log was omitted from subsequent correlation evaluations. To aid in the correlations, the gamma ray survey log (GR) was used as a screening tool for development of linear-regression correlation relationships between ELAN log responses and SWC porosity measurements. This helps account for the shale or clay content that can cause the inclusion of "bound water" porosity. To assign model layer porosities, the regression model relationships used to calibrate the ELAN measurement results (Figure 8-(Figure 3.9)) were applied to the ELAN survey results over the formational depths represented by the Mount Simon (3,918 to 4,430 ft) and overlying Eau Claire-Elmhurst member (3,852 to 3,918 ft) based on the gamma response criteria. The ELAN survey results are reported at 0.5-ft depth intervals. For stratigraphic units above the Elmhurst and/or depth intervals exhibiting gamma readings>64 API units, the uncalibrated, average ELAN log result for that depth interval was used. An average porosity was then assigned to the model layer based on the average of the calibrated ELAN values within the model layer depth range. Figure 9 (Figure 3.10) shows the depth profile of the assigned model layer porosities based on the average of the calibrated ELAN values. The actual values assigned for each layer are listed in Table 1.

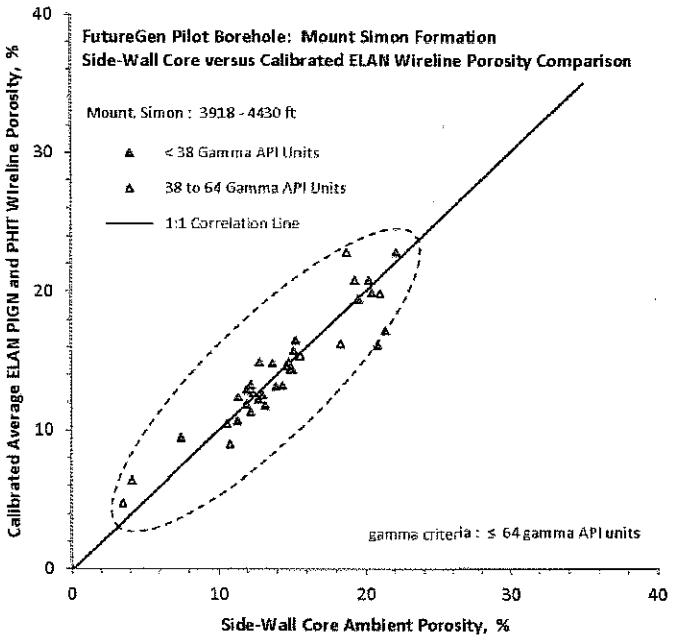

Comparison of SWC Porosity Measurements and Regression-Calibrated ELAN Log Porosities: ≤64 Gamma API Units

Figure 8

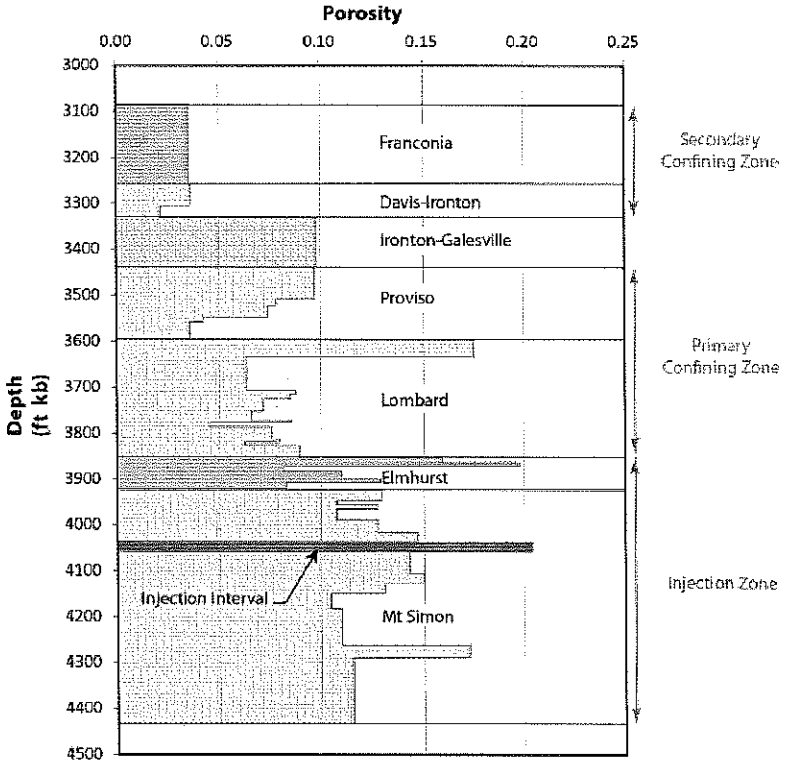

Figure 3.10. Porosity Versus Depth in Each Model Layer

Figure 9

3.3 *Rock (bulk) Density and Grain Density*

Grain density data were calculated from laboratory measurements of SWCs. The data were then averaged (arithmetic mean) for each main stratigraphic layer in the model. Only the Proviso member (Eau Claire Formation) has been divided in two sublayers to be consistent with the lithology changes. Figure 10 (Figure 3.11) shows the calculated grain density with depth. The actual values assigned to each layer of the model are listed in Table 1. Grain density is the input parameter specified in the simulation input file, and STOMP-CO2 calculates the bulk density from the grain density and porosity for each model layer.

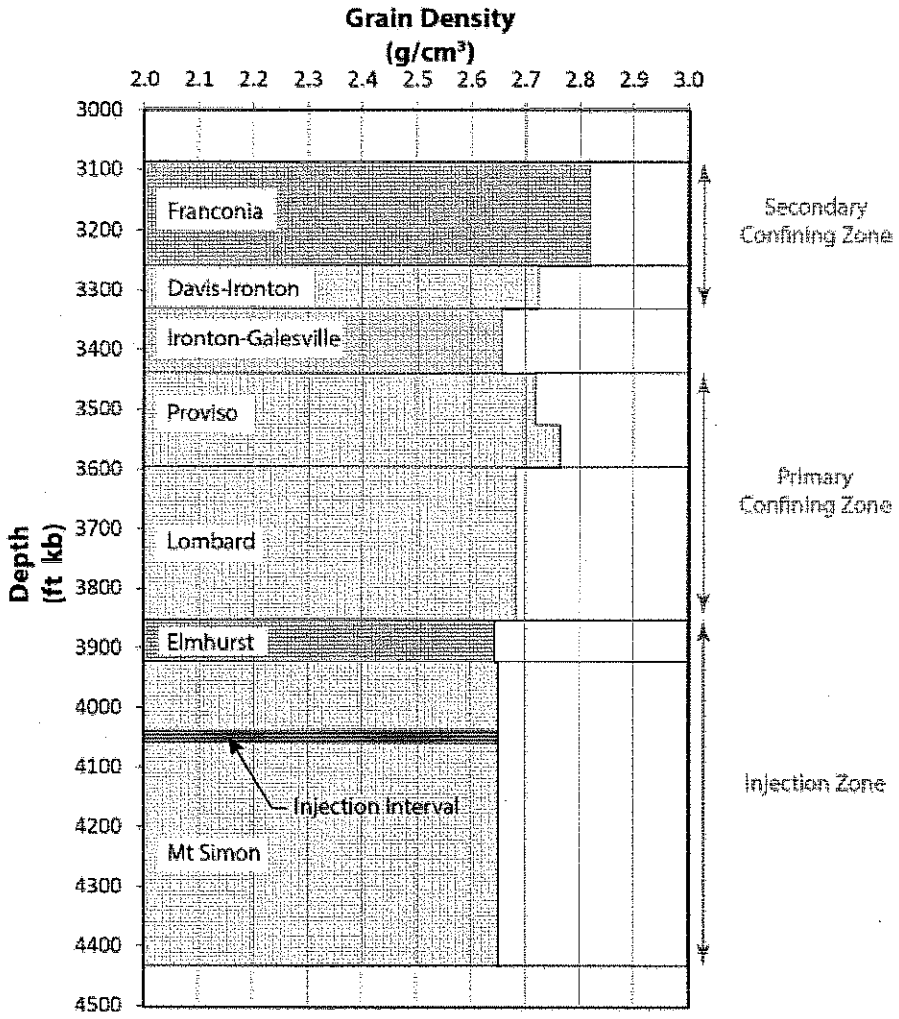

Figure 3.11. Grain Density Versus Depth in Each Model Layer

Figure 10

3.4 *Formation compressibility*

Limited information about formation (pore) compressibility estimates is available. The best estimate for the Mount Simon Sandstone (Table 2 (Table 3.7)) is that back-calculated by Birkholzer et al. (2008) from a pumping test at the Hudson Field natural-gas storage site, found 80 mi (129 km) northeast of the Morgan County CO_2 storage site. The back-calculated pore-compressibility estimate for the Mount Simon of 3.71E−10 Pa^{-1} was used as a spatially constant value for their basin-scale simulations. In other simulations, Birkholzer et al. (2008) assumed a pore-compressibility value of 4.5E−10 Pa^{-1} for aquifers and 9.0E−10 Pa^{-1} for aquitards. Zhou et

al. (2010) in a later publication used a pore-compressibility value of 7.42E−10 Pa^{-1} for both the Eau Claire Formation and Precambrian granite, which were also used for these initial simulations (Table 2). Because the site-specific data are limited to a single reservoir sample, only these two published values have been used for the model. The first value (3.71E-10 Pa^{-1}) has been used for sands that are compressible because of the presence of porosity. The second value (7.42E-10 Pa^{-1}) is assigned for all other rocks that are less compressible (dolomite, limestone, shale, and rhyolite). Table 1 lists the hydrologic parameters assigned to each model layer.

Table 2

Table 3.5. Permeability Ranges Used to Assign Brooks-Corey Parameters to Model Layers

Permeability (mD)	Psi (ψ)	Lambda (λ)	Residual Aqueous Saturation
< 41.16	4.116	0.83113	0.059705
41.16 to 231	1.573	0.62146	0.081005
231 to 912.47	1.450	1.1663	0.070762
> 912.47	1.008	1.3532	0.044002

3.5 Constitutive Relationships

3.5.1 Capillary pressure and saturation functions

Capillary pressure is the pressure difference across the interface of two immiscible fluids (e.g., CO_2 and water). The entry capillary pressure is the minimum pressure required for an immiscible non-wetting fluid (i.e., CO_2) to overcome capillary and interfacial forces and enter pore space containing the wetting fluid (i.e., saline formation water). Capillary pressure data determined from site-specific cores were not available at the time the model was constructed. However, tabulated capillary pressure data were available for several Mount Simon gas storage fields in the Illinois Basin. The data for the Manlove Hazen well (FutureGen Alliance, 2006) were the most complete. Therefore, these aqueous saturation and capillary pressure values were plotted and a user-defined curve fitting was performed to generate Brooks-Corey parameters for four different permeabilities (Figure 11- (Figure 3.12)). These parameters were then assigned to layers based on a permeability range as shown in Table 3 (Table 3.5).

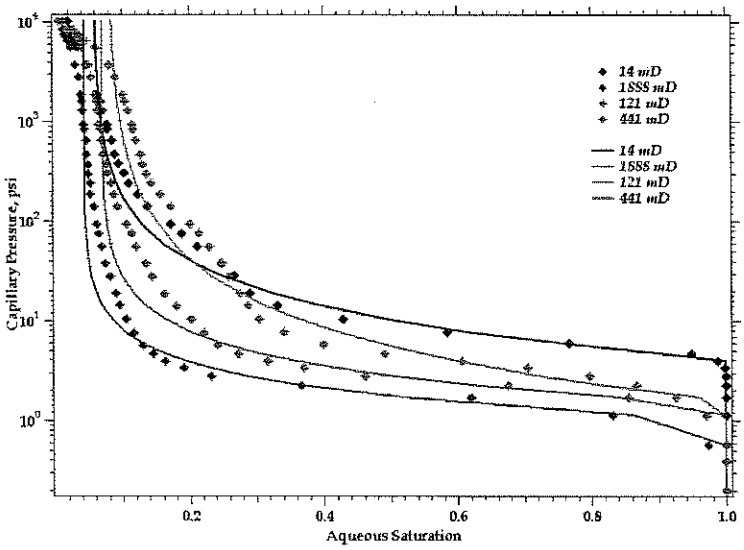

Aqueous Saturation Versus Capillary Pressure Based on Mercury Injection Data from the Hazen No. 5 Well at the Manlove Gas Field in Champagne County, Illinois

Figure 11

Table 3

Table 3.9. Pressure Data Obtained from the Mount Simon Formation Using the MDT Tool. (Red line delimits the samples within the injection zone.)

Sample Number	Sample Depth (ft bkb)	Absolute Pressure (psia)
7	4130	1828
8	4131	1827.7
9	4110.5	1818.3
11	**4048**	**1790.2**
17	**4048 (duplicated)**	**1790.3**
21	4248.5	1889.2
22	4246	1908.8
23	4263	1896.5[a]

(a) Sample affected by drilling fluids (not representative)

The Brooks-Corey (1964) saturation function is given as

$$S_{ew} = \begin{cases} (P_e / P_c)^{\lambda} & if \quad P_c > P_e \\ 1 & otherwise \end{cases}$$

where S_{ew} is effective aqueous saturation, P_c is capillary pressure, P_e is gas entry pressure, and λ is the pore-size distribution parameter. Combined with the Burdine (1953) relative permeability model, the relative permeability for the aqueous phase, k_{rw}, and that for the non-aqueous phase, k_{rn}, are

$$K_{rw} = (S_{ew})^{3+2/\lambda}$$

$$K_{rn} = (1 - S_{ew})^2 (1 - S_{ew}^{1+2/\lambda})$$

Values for the residual aqueous saturation (S_{rw}) and the two other parameters used in the Brooks-Corey capillary pressure-saturation function (i.e. the non-wetting fluid entry pressure and a pore-size distribution parameter) were all obtained by fitting mercury (Hg) intrusion-capillary pressure data from the Manlove gas storage site in Champaign County. The fitting was applied after scaling the capillary pressures to account for the differences in interfacial tensions and contact angles for the brine-CO2 fluid pair, relative to vapor-liquid Hg used in the measurements. This approach has the major advantage that the three fitted parameters are consistent as they are obtained from the same original data set. The use of consistent parameter values is not the norm for brine-CO2 flow simulations in the Mt. Simon.

The S_{rw} values used in the modeling (Table 2) are indeed lower than the values found in the literature. The FutureGen Alliance was aware about these differences but opted to use a consistent data set for all retention parameter values instead of selecting parameter values from different data sources. An additional reason for using this approach is the considerable uncertainty in S_{rw} values for Mt. Simon rock in the literature. In general, using a lower S_{rw} value for the injection zone will possibly result in a somewhat smaller predicted CO2 plume size and a smaller spatial extent of the pressure front compared to using a higher value of S_{rw}. Variation of S_{rw} in the confining zone (cap rock) likely has relatively little impact on CO2 transport and pressure development owing to the typically much lower permeability of this zone relative to the underlying reservoir.

3.5.2 Gas entry pressure

No site-specific data were available for gas entry pressure; therefore, this parameter was estimated using the Davies (1991) developed empirical relationships between air entry pressure, P_e, and intrinsic permeability, k, for different types of rock:

$$P_e = a\,k^b$$

where P_e takes the units of MPa and k the units of m^2, a and b are constants and are summarized below for shale, sandstone, and carbonate (Davies 1991; Table 3 (Table 3.6)). The dolomite found at the Morgan County site is categorized as a carbonate. The P_e for the air-water system is further converted to that for the CO_2-brine system by multiplying the interfacial tension ratio of a CO_2-brine system β_{cb} to an air-water system β_{aw}. An approximate value of 30 mN/m was used for β_{cb} and 72 mN/m for β_{aw}.

3.5.3 CO_2 entrapment

The entrapment option available in STOMP-CO2 was used to allow for entrapment of CO_2 when the aqueous phase is on an imbibition path (i.e., increasing aqueous saturation). Gas saturation can be free or trapped:

$$s_g = 1 - s_l = s_{gf} + s_{gt}$$

where the trapped gas is assumed to be in the form of aqueous occluded ganglia and immobile. The potential effective trapped gas saturation varies between zero and the effective maximum trapped gas saturation as a function of the historical minimum value of the apparent aqueous saturation. No site-specific data were available for the maximum trapped gas saturation, so this value was taken from the literature. Suekane et al. (2009) used micro-focused x-ray CT to image a chip of Berea Sandstone to measure the distribution of trapped gas bubbles after injection of $scCO_2$ and then water, under reservoir conditions. Based on results presented in the literature, a value of 0.2 was used in the model, representing the low end of measured values for the maximum trapped gas saturation in core samples.

4. Reservoir Properties

4.1 Fluid pressure

An initial fluid sampling event from the Mount Simon Formation was conducted on December 14, 2011 in the stratigraphic well during the course of conducting open-hole logging. Sampling was attempted at 22 discrete depths using the MDT tool in the Quicksilver Probe configuration and from one location using the conventional (dual-packer) configuration. Pressure data were obtained at 7 of the 23 attempted sampling points, including one duplicated measurement at a depth of 4,048 ft bkb (Table 4-(Table 3.9)).

Regionally, Gupta and Bair (1997) presented borehole drill-stem test (DST) data that indicated hydraulic heads within the Mount Simon Sandstone are near hydrostatic levels. Pressure depth measurements for the Mount Simon at the FutureGen stratigraphic well indicate a similar condition with a pressure gradient of ~0.4375 psi/ft, which is slightly higher than hydrostatic conditions (0.4331 psi/ft). Gupta and Blair (1997) also modeled the seepage velocity and flow direction of groundwater in the Mount Simon Formation across an eight-state area that does not include the Morgan County area, but does include eastern Illinois. They concluded that for deep bedrock aquifers, the lateral flow patterns are away from regional basin highs arches, such as the Kankakee Arch, and toward the deeper parts of the Illinois Basin. With respect to vertical groundwater flow, Gupta and Blair (1997) surmised that within the deeper portions of the Illinois Basin, groundwater has the potential to flow vertically upward from the Mount Simon to the Eau Claire, and the vertical velocities are <0.01 in./yr. They estimated that 17 percent of the water recharging the Mount Simon basin-wide migrates regionally into the overlying Eau Claire, while

83 percent flows laterally within the Mount Simon hydrogeologic unit. Vertical flow potential at the FutureGen site was evaluated based on an analysis of discrete pressure/depth measurements obtained within the pilot characterization borehole over the depth interval of 1,148 to 4,263 ft. The results indicate that there is a positive head difference in the Mount Simon that ranges from 47.8 to 61.6 ft above the calculated St. Peter observed static hydraulic head condition (i.e., 491.1 ft above MSL). This positive head difference suggests a natural vertical flow potential from the Mount Simon to the overlying St. Peter if hydraulic communication is afforded (e.g., an open communicative well). It should also be noted, however, that the higher head within the unconsolidated Quaternary aquifer (~611 ft above MSL), indicates a downward vertical flow potential from this surficial aquifer to both underlying St. Peter and Mount Simon bedrock aquifers The disparity in the calculated hydraulic head measurements (together with the significant differences in formation fluid salinity) also suggests that groundwater within the St. Peter and Mount Simon bedrock aquifers is physically isolated from one another. This is an indication that there are no significant conduits (open well bores or fracturing) between these two formations and that the Eau Claire forms an effective confining layer.

Note: Permit applicants did not provide the regional groundwater flow map that shows groundwater flow direction. However, they indicated that the modeling results of Gupta and Blair (1997) in the Mount Simon formation that does not include the Morgan County area showed that for deep bedrock aquifers, the lateral flow patterns are away from regional basin highs arches.

Table 4

Table 3.10. Summary of Initial Conditions

Parameter	Reference Depth (bkb)	Value
Reservoir Pressure	4,048 ft	1,790.2 psi
Aqueous Saturation		1.0
Reservoir Temperature	3,918 ft	96.6 °F
Temperature Gradient		0.00672 °F/ft
Salinity		47,500 ppm

4.2 Temperature

The best fluid temperature depth profile was performed on February 9, 2012 as part of the static borehole flow meter/fluid temperature survey that was conducted prior to the constant-rate injection flow meter surveys. Two confirmatory discrete probe depth measurements that were taken prior to the active injection phase (using colder brine) corroborate the survey results. The discrete static measurement for the depth of 3,712 ft was 95.9°F. The second discrete static probe temperature measurement is from the MDT probe for the successful sampling interval of 4,048 ft. A linear-regression temperature/depth relationship was developed for use by modeling. The regression data set analyzed was for temperature data over the depth interval of 1,300 to 4,547 ft. Based on this regression a projected temperature for the reference datum at the top of the Mount Simon (3,918 ft bkb) of 96.60°F is indicated. A slope (gradient) of 6.72×10^{-3} °F/ft and intercept of 70.27°F is also calculated from the regression analysis.

4.3 Brine density

Although this parameter is determined by the simulator using pressure, temperature, and salinity, based on the upper and lower Mount Simon reservoirs tests, the calculated in situ reservoir fluid density is 1.0315 g/cm^3.

4.4 Salinity and Water quality

During the process of drilling the well, fluid samples were obtained from discrete-depth intervals in the St. Peter Formation and the Mount Simon Formation using wireline-deployed sampling tools (MDTs) on December 14, 2011. After the well had been drilled, additional fluid samples were obtained from the open borehole section of the Mount Simon Formation by extensive pumping using a submersible pump. The assigned salinity value for the Mount Simon (upper zone) 47,500 ppm is as indicated by both the MDT sample (depth 4,048 ft) and the multiple samples collected during extensive composite pumping of the open borehole section.
A total of 20 groundwater samples were collected between October 25 and November 10, 2011, including duplicate samples and blanks (Dey et al. in press). General water-quality parameters were measured along with organic and major inorganic constituents. Values of pH ranged from 7.08 to 7.66. Values for specific conductance ranged from 545 to 1,164 µS/cm, with an average of 773 µS/cm. Values of Eh ranged from 105 to 532 mV with an average of 411 mV. Values of dissolved oxygen (DO) ranged from below detection limit to 3.3 mg/L O_2. Most dissolved inorganic constituent concentrations are within primary and secondary drinking water standards. However, the constituent concentration in water is elevated with respect to iron (Fe), manganese (Mn), nitrate (NO_3), and TDS. In some cases these constituents exceed the EPA secondary standards.

4.5 Fracture pressure in the injection zone

No hydraulic fracturing test has been conducted in the stratigraphic well and no site-specific fracture pressure values are available for the confining zone and the reservoir. Other approaches (listed below) have thus been chosen to determine an appropriate value for the fracture pressure.

- The geomechanical uncalibrated anisotropic elastic properties log from Schlumberger performed in the stratigraphic well could give information about the minimum horizontal stress. However, several assumptions are made and a calibration with available mini-fracs or leak-off tests is usually required to get accurate values of these elastic parameters for the studied site. These data will not be considered here.

- Triaxial tests were also conducted on eight samples from the stratigraphic well. Samples 3 to 7 are located within the injection zone. Fracture gradients were estimated to range from 0.647 to 0.682 psi/ft, which cannot directly be compared to the fracture pressure gradient required for the permit. Triaxial tests alone cannot provide accurate measurement of fracture pressure.

- Existing regional values. Similar carbon storage projects elsewhere in Illinois (in Macon and Christian counties) provide data for fracture pressure in a comparable geological context. In Macon County (CCS#1 well at Decatur), about 65 mi east of the FutureGen 2.0 proposed site, a fracture pressure gradient of 0.715 psi/ft was obtained at the base of the Mount Simon Sandstone Formation using a step-rate injection test (EPA 2011b). In Christian County, a "conservative" pressure gradient of 0.65 psi/ft was used for the same injecting zone (EPA 2011c). No site-specific data were available.

- Last, the regulation relating to the "Determination of Maximum Injection Pressure for Class I Wells" in EPA Region 5 is based on the fracture closure pressure, which has been chosen to be 0.57 psi/ft for the Mount Simon Sandstone (EPA 1994).

Based on all of these considerations, a fracture pressure gradient of 0.65 psi/ft was chosen. The EPA GS Rule requires that "Except during stimulation, the owner or operator must ensure that

injection pressure does not exceed 90 percent of the fracture pressure of the injection zone(s) so as to ensure that the injection does not initiate new fractures or propagate existing fractures in the injection zone(s)..." Therefore, a value of .585 psi/ft (90% of 0.65 psi/ft) was used in the model to calculate the maximum injection pressure

4.6 Site Evaluation of mineral resources

Other subsurface geochemical considerations include the potential for mineral or hydrocarbon resources beneath the proposed CO_2 storage site. While no significant mineral deposits are known to exist within Morgan County, natural gas has been recovered in the region, including at the Prentice and Jacksonville fields located within several miles of the stratigraphic well. ISGS oil and gas website data indicate that the Prentice Field contained more than 25 wells drilled during the 1950s; re exploration occurred in the 1980s. Both oil and gas have been produced from small stratigraphic traps in the shallow Pennsylvanian targets, at depths of 250 to 350 ft (75 to 105 m) bgs. It is important to note that gas produced from these wells may contain around 16 percent CO_2 (Meents 1981). More than 75 wells have been drilled in the Jacksonville Field. Gas was discovered in the Jacksonville Field as early as 1890 (Bell 1927), but most oil and gas production from the Prentice and Jacksonville fields occurred between the late 1920s and late 1980s. The most productive formations in the Illinois Basin (lower Pennsylvanian and Mississippian siliciclastics and Silurian reefs) are not present in Morgan County. Only two boreholes in the vicinity of the Prentice Field and five boreholes near the Jacksonville Field penetrate through the New Albany Shale into Devonian and Silurian limestones. Cumulative production from the Prentice and Jacksonville fields is not available, and both fields are largely abandoned. The Waverly Storage Field natural-gas storage site in the southeast corner of Morgan County originally produced oil from Silurian carbonates. This field no longer actively produces oil, but since 1954 it has been successfully used for natural-gas storage in the St. Peter and the Galesville/Ironton Sandstone formations (Buschbach and Bond 1974).

The nearest active coal mine is approximately 10 mi (16 km) away in Menard County and does not penetrate more than 200 ft (61 m) bgs (ISGS 2012a). A review of the known coal geology within a 5-mi (8-km) radius of the proposed drilling site indicates that the Pennsylvanian coals, the Herrin, Springfield, and Colchester coals, are very thin or are absent from the project area (ISGS 2010, 2011; Hatch and Affolter 2008). During continuous coring of a shallow groundwater monitoring well, immediately adjacent to the stratigraphic well, only a single thin (5-ft [1.5-m]) coal seam was encountered at about 200 ft (61 m) deep.

5. Initial Conditions

The reservoir is assumed to be under hydrostatic conditions with no regional or local flow conditions. Therefore the hydrologic flow system is assumed to be at steady state until the start of injection. To achieve this with the STOMP-CO2 simulator one can either run an initial simulation (executed for a very long time period until steady-state conditions are achieved) to generate the initial distribution of pressure, temperature, and salinity conditions in the model from an initial guess, or one can specify the initial conditions at a reference depth using the hydrostatic option, allowing the simulator to calculate and assign the initial conditions to all the model nodes. Site-specific data were available for pressure, temperature, and salinity, and therefore the hydrostatic option was used to assign initial conditions. A temperature gradient was specified based on the geothermal gradient, but the initial salinity was considered to be constant for the entire domain. A summary of the initial conditions is presented in Table 5 (Table 3.10).

Table 5

Table 2.17 List of Wells Located Within the AoR

Map ID	API Number	ISWS ID	Latitude NAD1983	Longitude NAD1983	Public Land Survey System	Total Depth ft	Elev ft	Completion Date	Owner	Well Num	Well Type	Status	Confining Zone Penetration Well	In AoR
0	[illegible]		39.800664	-90.052919	T16N,R9W,Sec 25	4812	633	TBD	FutureGen Industrial Alliance, Inc	1	Monitoring	Active	Yes	Yes
3	121372113200	116519	39.778074	-90.078443	T15N,R9W,Sec 2	25		19780712	A.A. Negus Estate	1	Water	Private Water Well	No	Yes
4	121370012700	115772	39.811025	-90.066241	T16N,R9W,Sec 25	115			Beilschmidt, William H		Water		No	Yes
8	121370028500	115740	39.800661	-90.072386	T16N,R9W,Sec 26	137		1950	Martin, L. E.	1	Water		No	Yes
9		115741	39.800661	-90.075386	T16N,R9W,Sec 26	127			Martin, L.E.		Water		No	Yes
10	121372126600	115779	39.801129	-90.07342	T16N,R9W,Sec 26	25		19781213	Martin, Marvin & Jean	1	Water	Private Water Well	No	Yes
14		115763	39.792894	-90.072875	T16N,R9W,Sec 35	26			E Clemons		Water		No	Yes
15		115764	39.792894	-90.072875	T16N,R9W,Sec 35	25			B Sexter		Water		No	Yes
16		115765	39.792837	-90.060298	T16N,R9W,Sec 36	35			J M Dugan		Water		No	Yes
17	121370051100		39.792893	-90.076984	T16N,R9W,Sec 35	1056	643		O'Sear, Judge	1	Oil & Gas / Water		No	Yes
18	121370009900		39.806545	-90.06615	T16N,R9W,Sec 25	1530	636	19390101	Beilschmidt, Wm.	1	Oil & Gas	Dry and Abandoned, No Shows	No	Yes
19	121370023500		39.779153	-90.077325	T15N,R9W,Sec 2	335	644	19231101	Conklin	1	Oil & Gas	Dry and Abandoned, No Shows	No	Yes
20	121370022600		39.781293	-90.075022	T15N,R9W,Sec 2	348	646	19231101	Conklin	2	Oil & Gas	Dry and Abandoned, No Shows	No	Yes
21	121370023700		39.778057	-90.080754	T15N,R9W,Sec 3	343	645	19231001	Harris, A. J.	1	Oil & Gas	Gas Producer	No	Yes
22	121370023900		39.7772	-90.080756	T15N,R9W,Sec 3	338	644	19231107	Harris, A. J.	2	Oil & Gas	Gas Producer	No	Yes
25	121370056300		39.805251	-90.075597	T16N,R9W,Sec 26	1205		19670330	Martin	1	Oil & Gas	Dry and Abandoned, No Shows	No	Yes
26	121370036300		39.806251	-90.075597	T16N,R9W,Sec 26	1400		19730329	Martin	1	Oil & Gas	Junked and Abandoned, Plugged	No	Yes
27	121372088500		39.800661	-90.073017	T16N,R9W,Sec 26	300	630				Coal Test		No	Yes
		115735	39.807336	-90.060378	T16N,R9W,Sec 25	25			Beilschmidt, William H		Water		No	Potentially
		115736	39.807336	-90.060378	T16N,R9W,Sec 25	30			W R Fowler		Water		No	Potentially
		115737	39.807336	-90.060378	T16N,R9W,Sec 25	25			Mason		Water		No	Potentially
		115739	39.807478	-90.079049	T16N,R9W,Sec 26	25			C H Mann		Water		No	Potentially
		115738	39.807478	-90.079049	T16N,R9W,Sec 26	22			T Goodall		Water		No	Potentially
		115650	39.807193	-90.041413	T16N,R8W,Sec 30	19		1938	R Allison		Water		No	Potentially
		115651	39.792765	-90.041512	T16N,R8W,Sec 31	28			W J Hasson		Water		No	Potentially
		115652	39.792765	-90.041512	T16N,R8W,Sec 31	28			F Robinson		Water		No	Potentially
		116456	39.777085	-90.052023	T15N,R9W,Sec 1	25			Al Harris		Water		No	Potentially
		116453	39.776968	-90.070521	T15N,R9W,Sec 2	32			A Harris		Water		No	Potentially
		116451	39.776968	-90.070521	T15N,R9W,Sec 2	22			W R Conklin		Water		No	Potentially
		116452	39.776968	-90.070521	T15N,R9W,Sec 2	30			B Negus		Water		No	Potentially
		116454	39.77688	-90.088996	T15N,R9W,Sec 3	26			C Negus		Water		No	Potentially
		116455	39.77688	-90.088996	T15N,R9W,Sec 3	30			L B Trotter		Water		No	Potentially
		115727	39.821851	-90.078925	T16N,R9W,Sec 23	30			D Sims		Water		No	Potentially
		115728	39.821851	-90.072925	T16N,R9W,Sec 23	30			Hazel Dell School		Water		No	Potentially
		115729	39.821851	-90.078925	T16N,R9W,Sec 23	35			K Haneline		Water		No	Potentially
		115733	39.821811	-90.060168	T16N,R9W,Sec 24	30			F L Icenogle		Water		No	Potentially
		115734	39.821811	-90.060168	T16N,R9W,Sec 24	30			G Lewis		Water		No	Potentially
		115775	39.821811	-90.060162	T16N,R9W,Sec 24	200		1944	E C Lewis		Water		No	Potentially
		115742	39.807531	-90.097566	T16N,R9W,Sec 27	23			J Stewart		Water		No	Potentially
		115743	39.807531	-90.097566	T16N,R9W,Sec 27	23			I J Stewart		Water		No	Potentially
		115761	39.792917	-90.097513	T16N,R9W,Sec 34	28			F Harrison		Water		No	Potentially
		115762	39.792917	-90.097513	T16N,R9W,Sec 34	30			J Mahon		Water		No	Potentially

6. *Boundary Conditions*

Boundary conditions were established with the assumption that the reservoir is continuous throughout the region and that the underlying Precambrian unit is impermeable. Therefore, the bottom boundary was set as a no-flow boundary for aqueous fluids and for the CO_2-rich phase. The lateral and top boundary conditions were set to hydrostatic pressure using the initial condition with the assumption that each of these boundaries is distant enough from the injection zone to have minimal to no effect on the CO_2 plume migration and pressure distribution.

7. *Wells Within the Survey Area*

A survey area of 25 mi^2 (65 km^2) that is centered on the proposed injection location and encompasses the area of the expected CO_2 plume (the AoR) is shown in Figure 12 (Figure 2.32). Surface bodies of water and other pertinent surface features (including structures intended for human occupancy), administrative boundaries, and roads are shown. There are no subsurface cleanup sites, mines, quarries, or Tribal lands within this area. Although numerous wells are located within a 25 mi^2 (65 km^2) survey area that includes the proposed injection location (Figure 1), none but the Alliance's stratigraphic well penetrates the injection zone (Mount Simon Sandstone and the lower Eau Claire [Elmhurst Sandstone Member]), the confining zone (Lombard and Proviso members of the Eau Claire Formation), or the secondary confining zone (Franconia Dolomite). A total of 129 wells (including stratigraphic well) are within the survey area (see Appendix B); 51 wells are (or are potentially) within the AoR (Table 6 – (Table 2.17)). Indeed, 24 of these 51 water wells are only identified with a general location (center of a section) in the ISWS database. If the section of those wells intersected the AoR borders, the wells were assumed to be within the AoR even though they could be beyond the border. Those well are indicated with a "potentially" label in the last column of the Table 6 but are not shown on the map. Shallow domestic water wells with depths of less than 50 ft (15 m) are the most common well type. Five slightly deeper water wells were identified that range in depths from 110 ft (33 m) to 405 ft (123 m). Other wells include stratigraphic test holes, coal test holes, and oil and gas wells (Figure 12). Table 6 lists these wells with their unique API (American Petroleum Institute) identification number, ISWS well identification (ID), well location, depth, elevation, completion

date, well owner, well type, and identified status. The map in Figure 12 shows the locations of four proposed injection wells for which permits are being sought. It also shows the location of the Alliance's stratigraphic well and abandoned hydrocarbon test holes, coal test holes, oil and gas wells, other plugged and abandoned wells, known water wells, and other surface features within a 25 mi^2 (65 km^2) area centered on the location of the proposed injection wells.

Table 6

Table 2.17. List of Wells Located Within the AoR

Map ID	API Number	KGS ID	Latitude NAD1983	Longitude NAD1983	Public Land Survey System	Total Depth ft	Elev ft	Completion Date	Owner	Well Num	Well Type	Status	Confining Zone Penetration Well	In AoR
[illegible]	[illegible]		[illegible]	[illegible]	[illegible]	[illegible]	[illegible]	TBD	[illegible] Industrial Alliance, Inc.	1	[illegible]	[illegible]	Yes	Yes
3	15137211838	116819	39.779174	-99.073445	T1S,R29W,Sec 2	25		19780712	A.A. Nagus Estate	1	Water	Private Water Well	No	Yes
[illegible]	[illegible]	[illegible]	[illegible]	[illegible]	[illegible]	[illegible]			[illegible]		Water		No	Yes
8	15137002595	115748	39.800661	-99.078326	T16S,R29W,Sec 26	117		1959	Martin, L.E.	1	Water		No	Yes
[illegible]		[illegible]	[illegible]	[illegible]	[illegible]	[illegible]			[illegible]		Water		No	Yes
10	15137212880	115779	39.801150	-99.07943	T16S,R29W,Sec 26	25		19781213	Martin, Mason & Jean	1	Water	Private Water Well	No	Yes
[illegible]		[illegible]	[illegible]	[illegible]	[illegible]	[illegible]			[illegible]		Water		No	Yes
15		115764	39.792698	-99.078375	T16S,R29W,Sec 35	25			B Sinex		Water		No	Yes
[illegible]		[illegible]	[illegible]	[illegible]	[illegible]	[illegible]			[illegible]		Water		No	Yes
17	15137005100		39.792695	-99.078086	T16S,R29W,Sec 35	1056	583		O'Kane, Judge	1	Oil & Gas / Water		No	Yes
[illegible]	[illegible]		[illegible]	[illegible]	[illegible]	[illegible]	[illegible]	[illegible]	[illegible]	1	Oil & Gas	Dry and Abandoned, No Shows	No	Yes
19	15137022500		39.779153	-99.077325	T1N,R29W,Sec 2	338	644	19231101	Conklin	1	Oil & Gas	Dry and Abandoned, No Shows	No	Yes
[illegible]	[illegible]		[illegible]	[illegible]	[illegible]	[illegible]	[illegible]	[illegible]	[illegible]	[illegible]	Oil & Gas	Dry and Abandoned, No Shows	No	Yes
21	15137002370		39.778407	-99.080754	T1N,R29W,Sec 3	342	655	19231002	Barry, A. I.	1	Oil & Gas	Gas Producer	No	Yes
[illegible]	[illegible]		[illegible]	[illegible]	[illegible]	[illegible]	[illegible]	[illegible]	[illegible]	[illegible]	Oil & Gas	Gas Producer	No	Yes
25	15137004555		39.806251	-99.073567	T16S,R29W,Sec 26	1209		19570330	Martin	1	Oil & Gas	Dry and Abandoned, No Shows	No	Yes
[illegible]	[illegible]		[illegible]	[illegible]	[illegible]	[illegible]		[illegible]	[illegible]	1	Oil & Gas	Plugged and Abandoned, Plugged	No	Yes
27	15137008505		39.800461	-99.073037	T16S,R29W,Sec 26	301	630				Coal Test		No	Yes
		[illegible]	[illegible]	[illegible]	[illegible]	[illegible]			[illegible]		Water		No	Potentially
		115734	39.807386	-99.060178	T16S,R29W,Sec 25	30			W E Fowler		Water		No	Potentially
		[illegible]	[illegible]	[illegible]	[illegible]	[illegible]			[illegible]		Water		No	Potentially
		115737	39.807478	-99.078989	T16S,R29W,Sec 26	25			C E Miller		Water		No	Potentially
		[illegible]	[illegible]	[illegible]	[illegible]	[illegible]			[illegible]		Water		No	Potentially
		115859	39.807185	-99.094415	T16S,R29W,Sec 30	19		1959	R. Adams		Water		No	Potentially
		[illegible]	[illegible]	[illegible]	[illegible]	[illegible]			[illegible]		Water		No	Potentially
		115852	39.791765	-99.041513	T16S,R28W,Sec 31	28			E Robinson		Water		No	Potentially
		[illegible]	[illegible]	[illegible]	[illegible]	[illegible]			[illegible]		Water		No	Potentially
		116453	39.778569	-99.076033	T1N,R29W,Sec 2	32			A Harris		Water		No	Potentially
		[illegible]	[illegible]	[illegible]	[illegible]	[illegible]			[illegible]		Water		No	Potentially
		116452	39.775962	-99.072621	T1N,R29W,Sec 2	30			E Nagus		Water		No	Potentially
		[illegible]	[illegible]	[illegible]	[illegible]	[illegible]			[illegible]		Water		No	Potentially
		116455	39.77488	-99.052966	T1N,R29W,Sec 3	30			L B Trotter		Water		No	Potentially
		[illegible]	[illegible]	[illegible]	[illegible]	[illegible]			[illegible]		Water		No	Potentially
		115728	39.821161	-99.071025	T16S,R29W,Sec 23	30			Hazel Dell School		Water		No	Potentially
		[illegible]	[illegible]	[illegible]	[illegible]	[illegible]			[illegible]		Water		No	Potentially
		115715	39.821821	-99.060168	T16S,R29W,Sec 24	30			J L Iseneyle		Water		No	Potentially
		[illegible]	[illegible]	[illegible]	[illegible]	[illegible]			[illegible]		Water		No	Potentially
		115775	39.821821	-99.060168	T16S,R29W,Sec 24	200		1944	E C Lewis		Water		No	Potentially
		[illegible]	[illegible]	[illegible]	[illegible]	[illegible]			[illegible]		Water		No	Potentially
		115743	39.807731	-99.097565	T16S,R29W,Sec 27	27			J J Stewart		Water		No	Potentially
		[illegible]	[illegible]	[illegible]	[illegible]	[illegible]			[illegible]		Water		No	Potentially
		115762	39.791917	-99.097513	T16S,R29W,Sec 34	30			J Mason		Water		No	Potentially

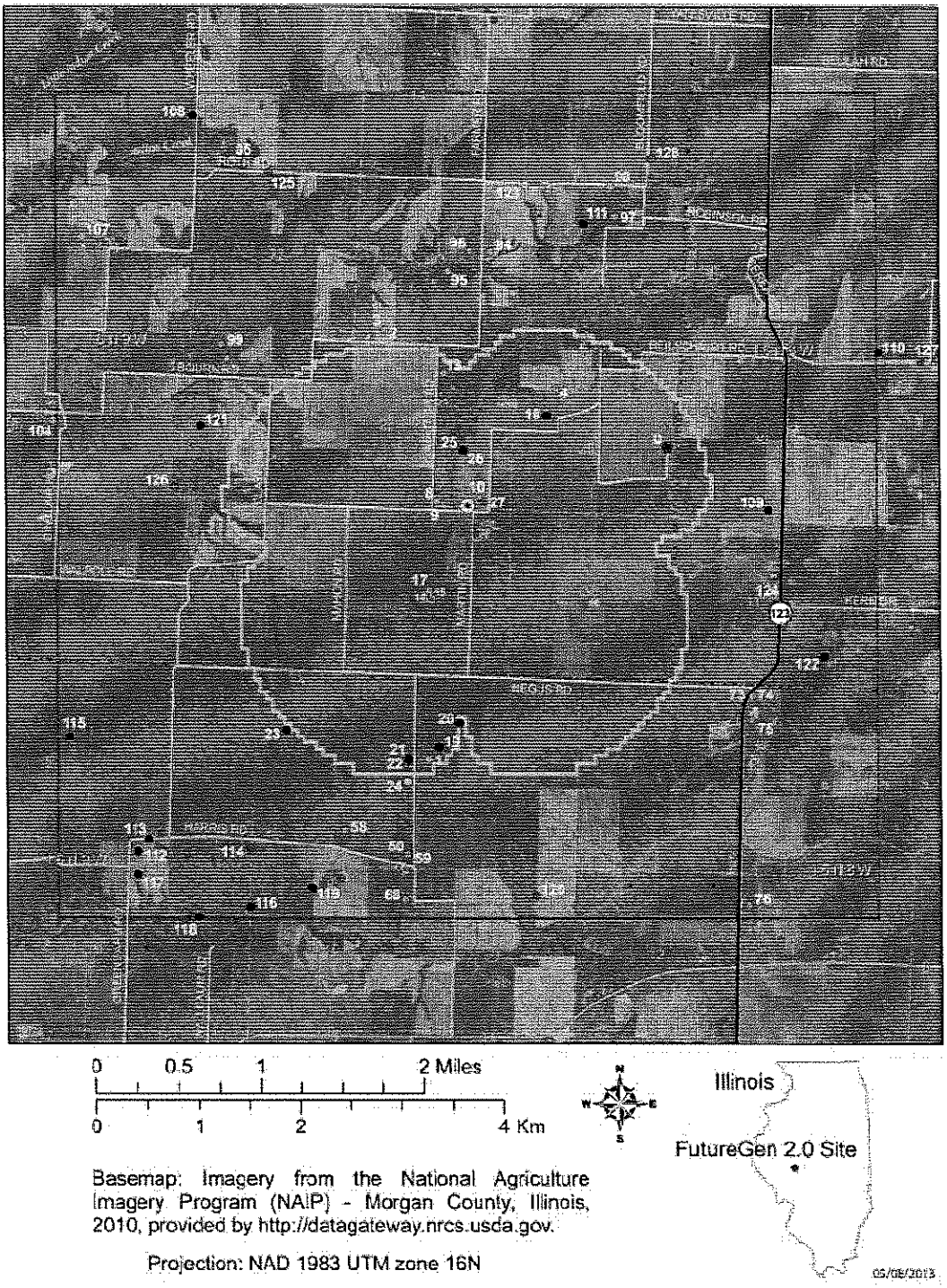

Figure 2.32. Wells Located Within the Survey Area. The map includes surface bodies of water, mines, quarries, faults, and other surface features. Tables of the data used to produce this map are provided in Table 2.17 and Appendix B.

Figure 12

8. *Proposed Operating Data (Operational Information)*

Figure 13 (Figure 3.18) shows the well design for the representative case for the refined area of the model domain in plan view and in 3D view. Injection into four lateral wells with a well-bore radius of 4.5 in. was modeled with the lateral leg of each well being located within the best layer of the injection zone to maximize injectivity. Only the non-cased open sections of the wells are specified in the model input file because only those sections are delivering CO_2 to the formation. The well design modeled in this case is the open borehole design, therefore part of the curved portion of each well is open and thereby represented in the model in addition to the lateral legs. The orientation and lateral length of the wells, as well as CO_2 mass injection rates, were chosen so that the resulting modeled CO_2 plume would avoid sensitive areas. The coordinates of the screened portion of the injection wells and the CO_2 mass injection rate was distributed among the four injection wells as shown in Table 7 and Table 8 (Table 3.11) for a total injection rate of 1.1 MMT/yr for 20 years. The injection rate was assigned to each well according to the values in Table 8. A maximum injection pressure of 2,252.3 psi was assigned at the top of the open interval (depth of 3,850 ft bgs), based on 90 percent of the fracture gradient described in Section 3.5 (0.65 psi/ft).

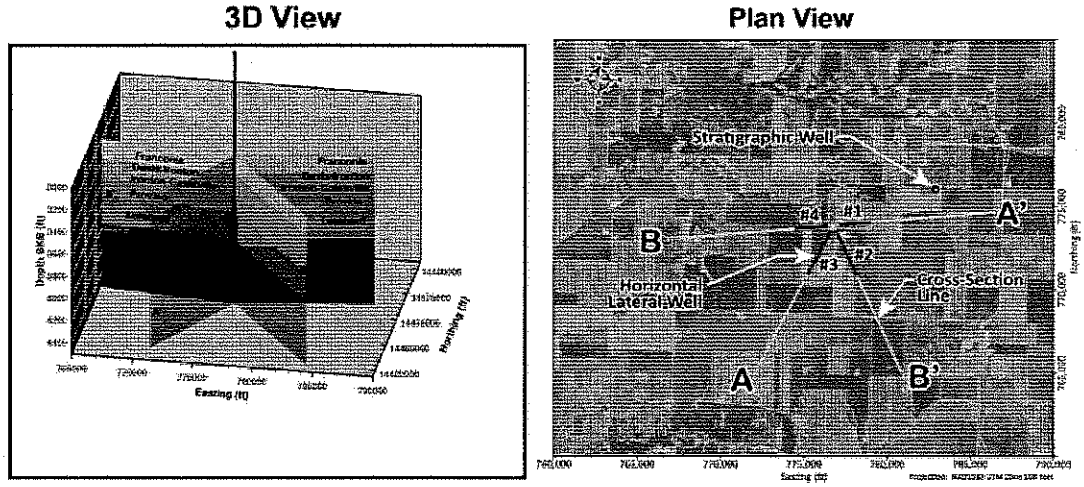

Figure 3.18. Operational Well Design for Representative Case Scenario as Implemented in the Numerical Model. The lateral legs of the injection wells are shown in red and the cross-section lines are shown in yellow.

Figure 13

Table 7. The coordinates of the screened portion of the injection wells

	Coordinate 1(ft)			Coordinate 2(ft)			Coordinate 3(ft)			Coordinate 4(ft)		
	x	y	z	x	y	z	x	y	z	x	y	z
Well 1	777079	14468885	-3200	777263	14468901	-3330	777592	14468929	-3392	779086	14469060	-3399
Well 2	776898	14468571	-3200	776976	14468404	-3330	777116	14468105	-3395	778172	14465839	-3463
Well 3	776617	14468578	-3200	776530	14468416	-3330	776375	14468124	-3389	775202	14465917	-3387
Well 4	776451	14468829	-3200	776267	14468813	-3330	775938	14468785	-3386	774444	14468654	-3379

Table 8

Table 3.11. Mass Rate of CO_2 Injection for Each of the Four Lateral Injection Wells

Well	Length of Lateral leg (ft)	Mass Rate of CO_2 Injection (MMT/yr)
Injection well #1	1,500	0.2063
Injection well #2	2,500	0.3541
Injection well #3	2,500	0.3541
Injection well #4	1,500	0.1856

9. *Computational Modeling Results*

At the end of the simulation period, 100 years, most of the CO_2 mass occurs in the CO_2-rich (or separate-) phase, with 20 percent occurring in the dissolved phase. Note that residual trapping begins to take place once injection ceases, resulting in about 15 percent of the total CO_2 mass being immobile at the end of 100 years. The CO_2 plume forms a cloverleaf pattern as a result of the four lateral injection-well design. The plume grows both laterally and vertically as injection continues. Most of the CO_2 resides in the Mount Simon Sandstone. A small amount of CO_2 enters into the Elmhurst and the lower part of the primary confining zone (Lombard). When injection ceases at 20 years, the lateral growth becomes negligible but the plume continues to move slowly primarily upward. Once CO_2 reaches the low-permeability zone in the upper Mount Simon it begins to move laterally. There is no additional CO_2 entering the confining zone from the injection zone after injection ceases.

9.1 Pressure front AOR delineation

Note: AOR delineation using the pressure front method is missing

9.2 Separate-phase plume AOR delineation

Using the CO_2-rich phase saturation as a defining parameter for the CO_2 plume extent is subject to overprediction due to numerical model choices such as grid spacing. Therefore, to accurately delineate the plume size, a methodology that used the vertically integrated mass per unit area (VIMPA) of CO_2 was developed. This ensures that the plume extent is defined based on the distribution of the mass of CO_2 in the injection zone. The VIMPA is calculated as follows:

$$VIMPA_{i,j} = \sum_{k} \frac{M_{i,j,k}}{A_{i,j,k}}$$

where M = the total CO_2 mass in a cell, A = the horizontal cross-sectional area of a cell, i and j = cell indices in the horizontal directions, and k = the index in the vertical direction.

For the purposes of AoR determination, the extent of the plume is defined as the contour line of VIMPA, within which 99.0 percent of the CO_2-rich phase (separate-phase) mass is contained. The acreage (areal extent in acres) of the plume is calculated by integrating all cells within the plume extent. Therefore, the CO_2 plume referred to in this document is defined as the area containing 99.0 percent of the separate phase CO_2 mass. After 20 years of injection and 2 years of shut-in, the areal extent of the separate-phase CO_2 plume no longer increases significantly. Therefore, the AoR, shown in Figure 14 (Figure 3.25), is delineated based on the predicted areal extent of the separate-phase CO_2 plume at 22 years.

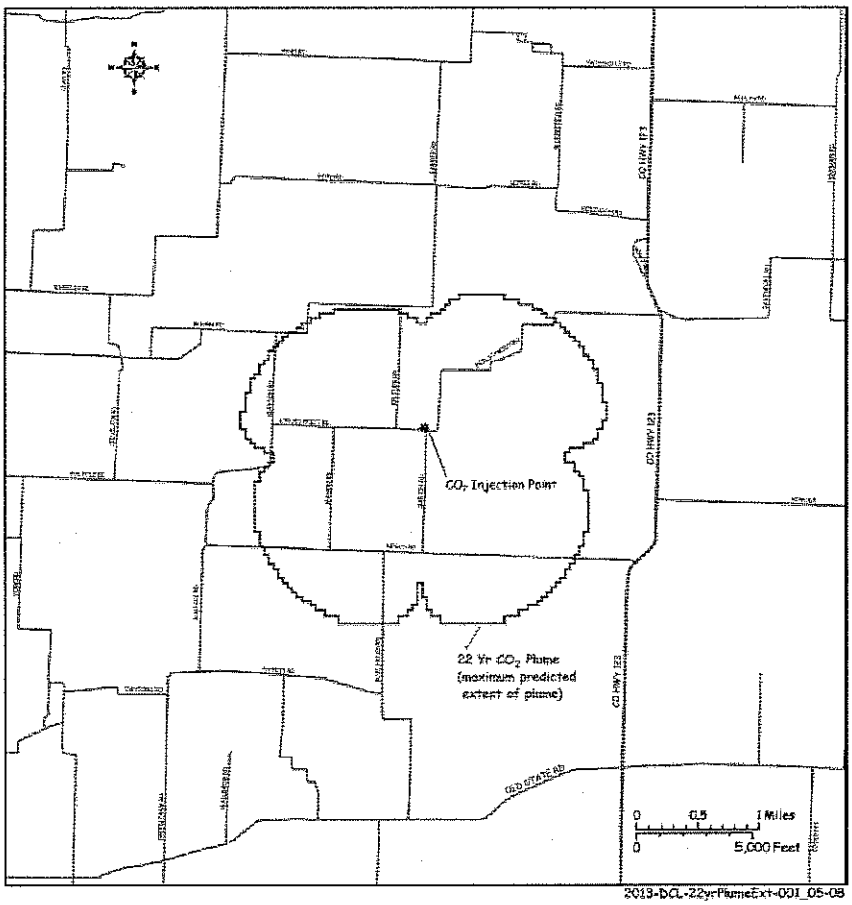

Figure 3.25. Area of Review for the Morgan County CO_2 Storage Site

Figure 14

Corrective Action Plan and Schedule

Area of Review Reevaluation Plan and Schedule

Proposed Reevaluation Cycle

The Alliance will reevaluate the AoR, at a minimum, every 5 years after issuance of a UIC Class VI permit and initiation of injection operations, as required by 40 CFR 146.84(b)(2)(i).

Although the Alliance will reevaluate the AoR every 5 years, some conditions would warrant reevaluation prior to the next scheduled reevaluation. These conditions include

1) A significant change in operations such as a prolonged increase or decrease in the CO_2 injection rates at the injections wells

2) A significant difference between simulated and observed pressure and CO_2 arrival response at site monitoring wells

3) Newly collected characterization data that have a significant effect on the site computational model.

Reevaluation Strategy

If any of these conditions occurs, the Alliance will reevaluate the AoR as described below. Ongoing direct and indirect monitoring data, which provide relevant information for understanding the development and evolution of the CO_2 plume, will be used to support

reevaluation of the AoR. These data include 1) the chemical and physical characteristics of the CO_2 injection stream based on sampling and analysis; 2) continuous monitoring of injection mass flow rate, pressure, temperature, and fluid volume; 3) measurements of pressure response at all site monitoring wells; and 4) CO_2 arrival and transport response at all site monitoring wells based on direct aqueous measurements and selected indirect monitoring method(s). The Alliance will compare these observational data with predicted responses from the computational model and if significant discrepancies between the observed and predicted responses exist, the monitoring data will be used to recalibrate the model (Figure 15 –Figure 3.26). In cases where the observed monitoring data agree with model predictions, an AoR reevaluation will consist of a demonstration that monitoring data are consistent with modeled predictions. As additional characterization data are collected, the site conceptual model will be revised and the modeling steps described above will be repeated to incorporate new knowledge about the site.

Note: Provide additional information on quantative threshold that would trigger a revision of the AOR model (e.g. statistical differences between monitoring and modeling predictions, change in operations)

Provide a time Frame for reevaluation (e.g. within one month of detection)

Provide the seismic event or other emergency criteria as a reason for reevaluation

The Alliance will submit a report notifying the UIC Program Director of the results of this reevaluation. At that time, the Alliance will either 1) submit the monitoring data and modeling results to demonstrate that no adjustment to the AoR is required, or 2) modify its Corrective Action, Emergency and Remedial Response and other plans to account for the revised AoR. All modeling inputs and data used to support AoR reevaluations will be retained by the Alliance for 10 years.

To the extent that the reevaluated AoR is different from the one identified in this supporting documentation, the Alliance will identify all active and abandoned wells and underground mines that penetrate the confining zone (the Eau Claire Formation) in the reevaluated AoR and will perform corrective actions on those wells. As needed, the Alliance will revise all other plans, such as the Emergency and Remedial Response Plan, to take into account the reevaluated AoR and will submit those plans to the UIC Program Director for review and approval.

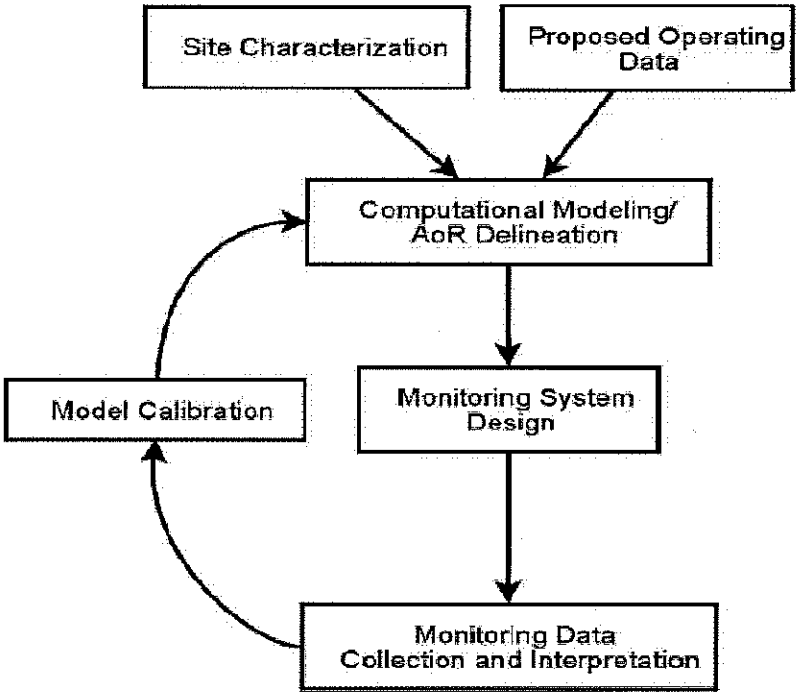

Figure 3.26. AoR Correction Action Plan Flowchart (from EPA 2011a)
Figure 15

References

FutureGen Alliance. 2006. Mattoon, Illinois Environmental Information Volume II Subsurface. PNWD-3768, prepared for the FutureGen Alliance by Battelle – Pacific Northwest Division, Richland, Washington.

White, S.P., R. Allis, J. Moore, T. Chidsey, C. Morgan, W. Gwynn, and M. Adams. 2005. Simulation of reactive transport of injected CO2 on the Colorado Plateau, Utah, USA. Chemical Geology 217:387–405.